Titre: Title:	Tannins for Green Electrochemical Energy Storage - A Comparative Study
Auteur: Author:	Alexandre Masson
Date:	2021
Type:	Mémoire ou thèse / Dissertation or Thesis
Référence: Citation:	Masson, A. (2021). Tannins for Green Electrochemical Energy Storage - A Comparative Study [Mémoire de maîtrise, Polytechnique Montréal]. PolyPublie. https://publications.polymtl.ca/9099/

POLYTECHNIQUE MONTRÉAL

affiliée à l'Université de Montréal

TANNINS FOR GREEN ELECTROCHEMICAL ENERGY STORAGE - A COMPARATIVE STUDY

ALEXANDRE MASSON

Département de génie physique

Mémoire présenté en vue de l'obtention du diplôme de *Maîtrise ès sciences appliquées*

Génie physique

Août 2021

POLYTECHNIQUE MONTRÉAL

affiliée à l'Université de Montréal

Ce mémoire intitulé :

TANNINS FOR GREEN ELECTROCHEMICAL ENERGY STORAGE - A COMPARATIVE STUDY

présenté par **Alexandre MASSON**

en vue de l'obtention du diplôme de *Maîtrise ès sciences appliquées*

a été dûment accepté par le jury d'examen constitué de :

Alain ROCHEFORT, président
Clara SANTATO, membre et directrice de recherche
Daniel BÉLANGER, membre externe

ACKNOWLEDGEMENTS

I wish to start by thanking Clara Santato for the countless opportunities she offered me during this thesis. You have been way more than a simple professor, you set an example and encouraged me to be autonomous and creative for this project, while always being a wise mentor and pointing me in the right direction.

I also want to gratefully acknowledge the immense help and tutoring that Abdelaziz Gouda gave me. You were always present to guide me in the lab, discuss new ideas and share important literature with me. This project is so much more than it would have been without you.

Olivier Girard also greatly contributed to the project by helping me with the SEM imaging. Thank you for your time at the microscope and your advice on the interpretation long after the end of the experiments.

Manuel and Anthony, you were great sources of inspiration and exceptional colleagues and friends, thank you for your advice, your encouragements and the useful articles you sent my way.

Finally, I would like to thank the members of the jury, Daniel Bélanger and Alain Rochefort, for taking the time to evaluate my work.

RESUME

Les préoccupations environnementales croissantes du début du siècle ont stimulé les investissements dans les énergies renouvelables et les véhicules électriques. L'intermittence des premières et l'abondance des seconds ont exercé une pression considérable sur la demande de stockage électrochimique de l'énergie. Les produits commerciaux actuels dépendent de matériaux inorganiques, entraînant des problèmes environnementaux et de disponibilité des ressources. La nécessité de développer des options basées sur des matériaux organiques, biosourcés et abondants est donc pressante, mais la faible conductivité et stabilité moyenne de la plupart des candidats ainsi que la difficulté de trouver un collecteur de courant efficace et sans métaux entravent leur développement.

Dans ce mémoire, nous étudions 5 représentants de la famille des tannins (catéchine, pyrogallol, acide tannique, epicatéchine, et gallate d'epicatéchine) et comparons leurs capacités de stockage de charge. Ces 5 tannins ont été choisis pour (i) la similarité de leurs structures : des polyphénols capables de s'oxyder de manière réversible en quinones, et (ii) leurs différences significatives, témoignant de la grande variété et du grand nombre de candidats de cette famille : taille, réactivité et complexité de la structure.

A partir de cet échantillon de 5 molécules, nous proposons une méthode générale pour évaluer et exploiter les propriétés de stockage d'énergie électrochimique des tannins. En exploitant la solubilité aqueuse de ces molécules, des solutions concentrées (eau/éthanol 2:1) de chaque tannin sont déposées sur des électrodes de carbone afin d'améliorer leur capacité de stockage par des processus d'oxydoréduction réversibles en surface.

L'électrode de carbone servant de substrat est préalablement traitée à l'aide d'une méthode d'activation acide et thermique afin d'augmenter sa surface et d'introduire un dopage de surface en O, N, S et P. L'augmentation de la surface améliore non seulement la capacité électrochimique à double couche de l'électrode de carbone sans tannins, mais permet également de déposer une couche plus fine de tannins pour la même masse totale, ce qui conduit à des processus limités en surface plutôt qu'en diffusion. Le dopage a pour effet combiné d'améliorer la mouillabilité, permettant ainsi l'accès à une plus grande partie de la surface du carbone et d'améliorer la pseudo-capacité de l'électrode en carbone sans tannins en introduisant des espèces électroactives. Cette

plus grande surface spécifique permet de compenser la faible conductivité électronique des molécules biosourcées et organiques telles que les tannins en favorisant la formation de dépôts plus minces et répartis.

Nous utilisons la microscopie électronique à balayage pour analyser la morphologie de surface de ces électrodes de carbone recouvertes de tannins. Nous évaluons ensuite leur potentiel de stockage de charge dans une cellule électrochimique à trois électrodes, en utilisant une grille de Pt comme contre-électrode et Ag/AgCl comme référence. La voltammétrie cyclique, la spectroscopie d'impédance électrochimique, ainsi que des mesures de charge et de décharge galvanostatique sont utilisées pour comparer les performances des 5 tannins.

La catéchine, le tannin le plus prometteur du point de vue de l'amélioration du stockage de charge et stabilité chimique est étudiée plus en profondeur. Un supercondensateur à base de catéchine et d'acide tannique (pour améliorer la stabilité du dispositif) est présenté dans un électrolyte aqueux à pH quasi-neutre (~ 6). Ce supercondensateur atteint 648 mF cm^{-2} (216 F g^{-1}), une efficacité coulombique de 100%, une rétention de capacité de plus de 100% après 5 000 cycles de charge/décharge, une densité de puissance maximale de 43 kW kg^{-1} et une densité d'énergie maximale de 54 Wh kg^{-1}. Ces valeurs font des tannins des candidats prometteurs à la fabrication de stockage électrochimique durable.

ABSTRACT

Growing environmental concerns spurred investment in intermittent renewable energies and electric vehicles placing a considerable stress on electrochemical energy storage demand. Current industrial standards are based on few, key, inorganic materials raising environmental and availability issues. Thus, the need to switch to biosourced, widely available, organic materials is pressing, but low conductivity and stability of most candidates and the difficulty to create efficient, metal-free current collectors hinder their development.

In this work, we focus on 5 quinone-based representatives of the tannin family (catechin, pyrogallol, tannic acid, epicatechin, and epicatechin gallate) and study their charge storage performance in electrochemical capacitor configuration using treated carbon electrodes. These 5 tannins were chosen for (i) their similar structures, characteristic of the tannin plant metabolites: polyphenols able to reversibly oxidize into quinones, and (ii) their significant differences, proof of the great variety of candidates in this family: size, reactivity, and complexity of the structure.

From this batch of molecules, we propose a general method to assess and exploit the electrochemical energy storage properties of tannins. Exploiting the aqueous solubility of these molecules, concentrated solutions (water/ethanol 2:1) of each tannin are drop casted on treated carbon electrodes to enhance their storage capacity through reversible surface redox processes.

The carbon electrode serving as substrate is initially treated using an acidic and thermal activation method to increase its surface area and introduce O, N, S, and P surface doping. The increased surface area not only improves the electrochemical double layer capacitance of the bare carbon electrode, but also allows for a thinner layer of tannins to be deposited for the same total mass, leading to surface limited instead of diffusion limited processes. The doping has a combined effect of improving the wettability, thus granting access to a greater portion of the surface of the carbon and enhancing the pseudocapacitance of the bare carbon electrode by introducing some electroactive functionalities. The larger specific surface area helps compensate for the low electronic conductivity of biosourced or organic molecules such as tannins by allowing thinner deposits.

We use scanning electron microscopy to analyze the surface morphology of these tannin-coated treated carbon electrodes. Afterwards, we assess their charge storage potential in a three-electrode

electrochemical cell, using Pt mesh as counter electrode and Ag/AgCl as reference. Cyclic voltammetry, electrochemical impedance spectroscopy, and galvanostatic charge and discharge are used to compare the performance of the 5 tannin candidates.

Catechin, the most promising tannin from the point of view of capacity enhancement and chemical stability is studied in device configuration. A catechin/tannic acid (to promote the cycling stability) symmetric aqueous electrochemical capacitor in near neutral electrolyte (pH ~ 6) is presented. This electrochemical capacitor exhibited a capacitance of 648 mF cm^{-2} (216 F g^{-1}), 100% Coulombic efficiency, over 100% capacitance retention after 5 000 charge/discharge cycles, 43 kW kg^{-1} maximal power density and 54 Wh kg^{-1} maximal energy density. These values make tannins promising candidates for green electrochemical energy storage.

TABLE OF CONTENTS

LIST OF TABLES

LIST OF FIGURES

LIST OF SYMBOLS AND ABBREVIATIONS

BET Brunauer, Emmett and Teller method

CV Cyclic Voltammetry

ELD Electric Double Layer

EDLC Electric Double Layer Capacitor

EDX Energy Dispersive X-ray spectroscopy

EIS Electrochemical Impedance Spectroscopy

GCD Galvanostatic Charge and Discharge

IHP Inner Helmholtz Plane

OHP Outer Helmholtz Plane

PVA Poly (Vinyl Alcohol)

SCR Space Charge Region

SEM Scanning Electron Microscopy

TCP Treated Carbon Paper

CHAPTER 1 INTRODUCTION

1.1 Context and motivation

The dawn of the 21st century has witnessed unprecedented efforts -- the Paris Agreement, government subsidies for clean energy, and the introduction of carbon taxes -- towards environmental sustainability as the world strives to achieve decarbonated and renewable energy [1]. Nonetheless, the most promising energy technologies -- solar- and wind-based -- to escape our fossil fuel dependence require energy storage capabilities to counterbalance their intermittent performance stemming from predictable but uncontrollable weather conditions.

All aspects of our modern way of life require electrical energy. World residential energy consumption has been growing steadily since the first industrial revolution and the last decades, despite environmental concerns, have failed to change the trend [2]. The development of electric vehicles to reduce greenhouse gas emissions increases electricity demand from the transportation field. Finally, the omnipresent digitalization symptomatic of the so-called fourth industrial revolution also adds on to the recent spur in energy storage demand [1].

The diversity of uses of electrical energy in our lives not only increases energy storage demand but requires a vast range of devices tailored to each application. Residential energy demand requires higher capacities but does not require portability, thus geothermal or hydroelectric storage options can be considered. Electric vehicles or portable consumer electronics require lightweight, high energy density devices. Lithium-ion batteries have conquered this market. Airplane emergency-exit doors that require reliable devices and high-power densities make use of electrochemical capacitors. Biosensors, e.g., for medical applications or soil monitoring, require small energy densities and should feature low human and environmental toxicity [3].

Electrochemical energy storage devices present the advantage of being very versatile and based on a great variety of materials [4]. However, commercially available electrochemical energy storage devices often rely on the use of materials with harmful effects on human health and whose extraction can have dramatic environmental and social impacts (such as cobalt) [5, 6]. Therefore, the need for new routes, e.g., based on more sustainable, biosourced redox-active organic materials,

is ever pressing. These alternative materials often present a quinone-hydroquinone redox active site, such as in melanins, lignin or tannins. This work focuses on the tannin family.

1.1.1 Applications of electrochemical capacitors

Batteries, electrolytic capacitors and electrochemical capacitors (or supercapacitors) are the three most common representatives of electrochemical energy devices [4]. Batteries present high energy densities (over 10 Wh kg^{-1} – see Figure 2.1) while capacitors (e.g. based on metals) deliver high power density (above 10^4 W kg^{-1}). Electrochemical capacitors present power and energy densities between those of electrolytic capacitors and batteries. They rely on very fast and reversible electrostatic processes making them highly reliable and granting them very long cycling lifetimes [7]. Their reliability has attracted attention in airplane security systems, military, and medical applications. Their long cycling life is exploited in electric vehicles to recover some of the braking energy to deliver it again during acceleration [3]. However, their low energy density (below 0.1 Wh kg^{-1}) limits their range of applications.

Electrochemical capacitors can combine electrostatic processes and faradaic surface reactions to achieve higher energy densities (up to 10 Wh kg^{-1}) while maintaining considerable power densities (up to 10^4 W kg^{-1}). They also present long cycling stability and, thanks to the attention they attracted in research, they are closing the energy density gap with batteries and could replace them in the future. Today electrochemical capacitors are used to regulate grid electricity fluxes or to power autonomous devices [4].

Carbon materials can be very low-cost and achieve very high surface area making them very interesting candidates for electrochemical capacitor applications [4]. Their compatibility with organic and/or biosourced materials is exploited to create high energy density electrochemical capacitors making use of redox-active molecules deposited on the surface of carbon electrodes [8].

1.1.2 Current uses for tannins

Tannins are present, at different concentrations, in most plants. They are a very diverse family comprising over a thousand molecules [9]. Their name stems from the Gaelic word *tan*, meaning

oak. Oak bark was used by ancient Welsh for leather tannin through the, at the time unknown, reducing effect of the tannins present in high concentration in this bark. We consume tannins everyday as they are naturally present in several basic food products. Tea leaves contain several types of tannins. They are responsible for the astringency of red wine. Catechin is highly concentrated in cocoa beans. Tannic acid is found abundantly in oak bark. Ancient Egyptians combined them with metallic ions to create colorful inks [10] and their anti-oxidant properties have been studied intensively for medicinal applications [11].

Tannins can be easily extracted from dry bark (see chapter 2.2) in which they are abundant. Today, large amounts of tannin-loaded bark are produced by the forest industry and considered waste often left on the ground. Rainwater has been shown to extract tannins from this waste, resulting in contamination and toxicity (reducing effects of tannins on minerals or metal cations) of nearby rivers or phreatic zones [12]. Tannins are polyphenol molecules with known redox activity.

1.2 Research objectives

This thesis aims to ascertain the use of tannins as biosourced materials for electrochemical energy storage. With this goal in mind, we focus on the following research objectives:

- Study the redox activity of selected tannins.
- Present a fabrication route for tannin-on-carbon electrodes.
- Evaluate the charge storage performance of electrochemical capacitor devices based on tannin-on-carbon electrodes.
- Identify the molecular characteristics of tannins most suitable to electrochemical energy storage applications.

1.3 Structure of the thesis

This Master of science thesis is structured in two main parts: a literature review on electrochemical capacitors tannins, and electroactive carbons and the case study of the use of tannins for electrochemical energy storage in electrochemical capacitor configuration. The first part of the literature review presents fundamental knowledge on the different processes contributing to the capacitance of electrochemical capacitors, namely electrostatic and faradaic reactions. The second part of the literature review focuses on tannins, presenting an overview of the molecule family and the past literature on tannins for electrochemical energy storage. The third and last part of the literature review presents the properties of electroactive carbons commonly used in electrochemical capacitor devices. The second part of the thesis is divided in 3 chapters. Chapter 3 details the experimental procedures, chapter 4 reports on tannins' redox activity, and chapter 5 evaluates their use in tannin-on-carbon electrochemical capacitors.

The detailed structure of the Master of Science thesis is as follows:

- Chapter 1 describes the context, motivation, and necessity for this work.
- Chapter 2 presents a literature review on the charge storage mechanisms of electrochemical capacitors, electroactive carbon, and the tannin family and its use in electrochemical energy storage.
- Chapter 3 details the experimental procedures and characterization methods.
- Chapter 4 explores the redox activity of tannins.
- Chapter 5 evaluates the charge storage performance of catechin-on-carbon based symmetric electrochemical capacitors in aqueous configuration.
- Chapter 6 concludes this work, discusses the challenges, and introduces possible perspectives.

CHAPTER 2 LITERATURE REVIEW

2.1 Electrochemical capacitors

2.1.1 Electrochemical energy storage devices

Intermittent renewable energies and electric vehicles require increasing energy storage capacities. Electrochemical energy storage devices are currently seen as the most promising options to address this critical growth in storage demand [1]. Indeed, they are low cost and can be tailored to diverse purposes. There are two main paths to store charges electrochemically: electrostatic and faradaic processes. The first is faster, more reversible while the second is slower but can store more charges [13].

Batteries and capacitors are the two main representatives of electrochemical energy storage [1]. Batteries are typically associated to bulk redox (faradaic) charge storage and capacitors to electrostatic forces [13]. They present complementary strengths, with batteries focusing on higher energy density, while capacitors offer high power density (Figure 2.1). Capacitors are used for their reliability, long cycling life (typically 500 000 cycles), fast discharge and high rate capability [4, 7, 14]. Electrochemical capacitors or electrochemical capacitors present a balanced option delivering power and energy densities between standard capacitors and batteries. For that they can make use of two (combinable) mechanisms: electrical double layer or pseudo-capacitance.

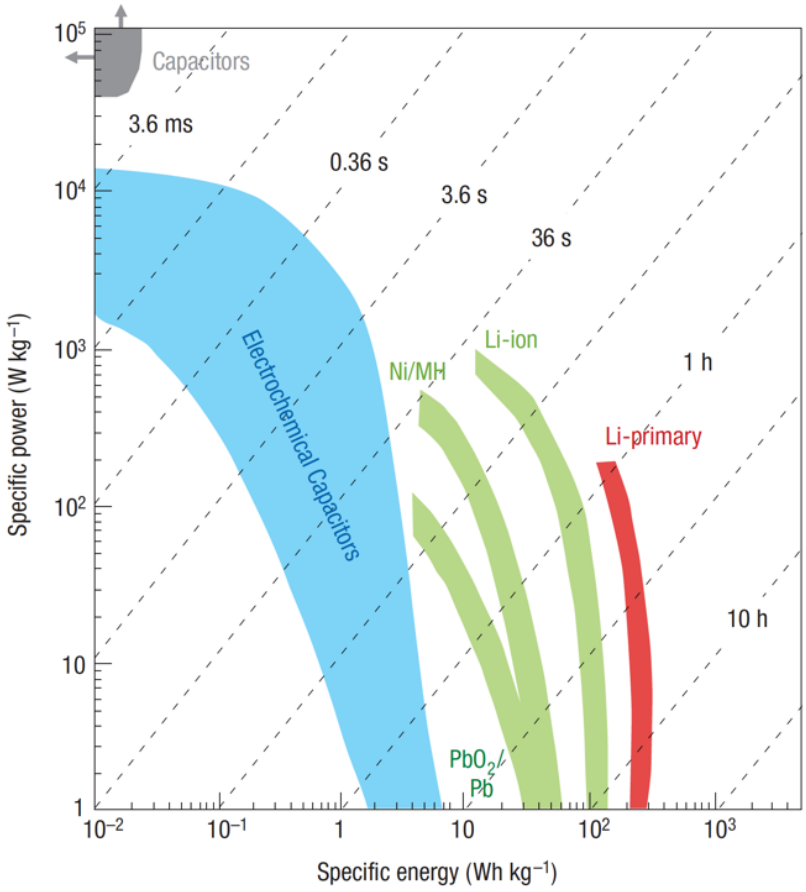

Figure 2.1 Ragone plot illustrating the performance difference between capacitors, batteries and electrochemical capacitors. Reproduced from [16].

2.1.2 Electrical double layer capacitors

Electrical double layer capacitors (EDLCs) exploit materials with very high surface areas to accumulate charges through purely electrostatic processes. The high specific surface area and high porosity of some carbon forms is of great interest for EDLCs. Further optimization and combination of micropores (< 2 nm), mesopores (2–50 nm), and macropores (> 50 nm) to maximize the surface accessibility of the electrolyte and minimize ion transport resistance can further improve the electrical double layer (EDL) capacitance. Carbon electrodes with specific surface area of over 2 000 $m^2\ g^{-1}$ can present specific capacitances exceeding 150–300 $F\ g^{-1}$ [4].

The specific capacitance of EDLCs is the result of three capacitive components in series: the space charge region (SCR) capacitance, the inner Helmholtz plane (IHP) capacitance and the outer Helmholtz plane (OHP) capacitance (Figure 2.2). The SCR is the result of a distribution of charge carriers in the bulk of an electrode upon its polarization. For semiconductors, the SCR ranges between 0.1 nm and 1 µm [15]. The IHP and OHP are formed in the electrolyte via ions compensating the electrode polarity. The IHP is formed very close to the interface, while the OHP corresponds to the larger diffuse layer of ions. The three capacitive components are the result of potential gradients due to this double layer of charge carriers at the electrode/electrolyte interface. It is simple to act on the SCR and OHP capacitances by increasing the conductivity of the electrode and the concentration of the electrolyte solution. Thus, it is usually the IHP capacitance that is the limiting contribution.

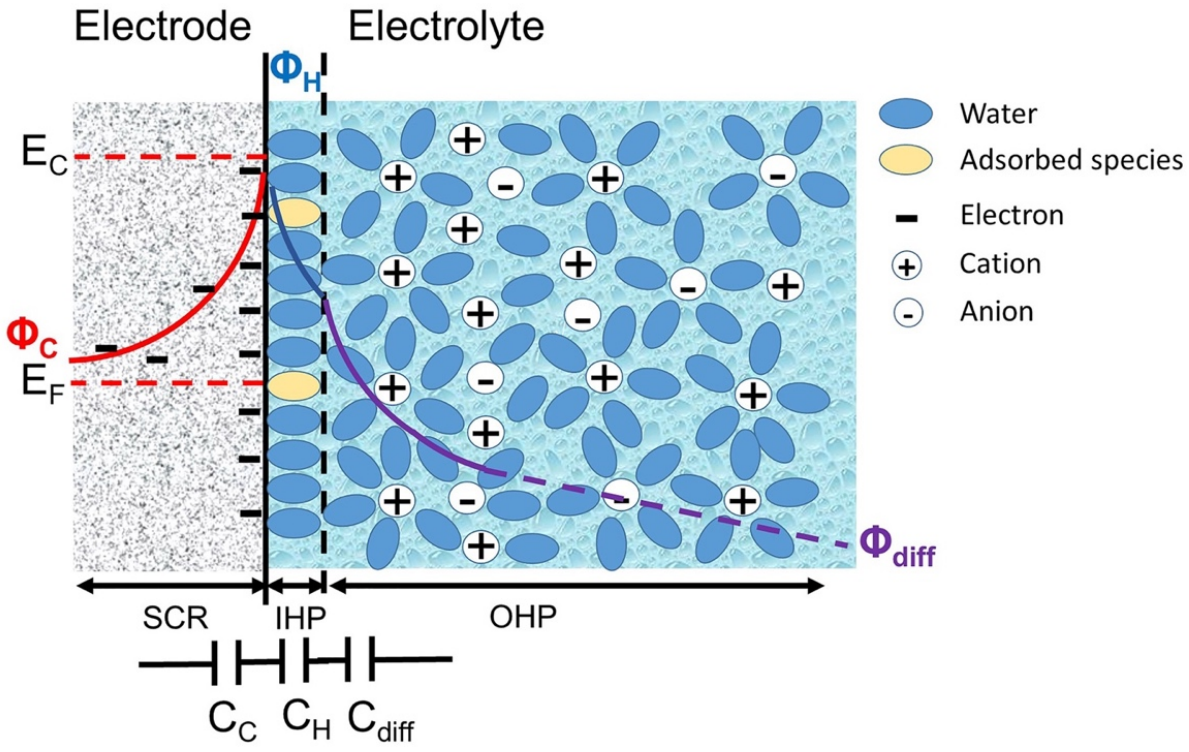

Figure 2.2 Scheme of an electrical double layer at a semiconducting electrode/electrolyte interface. C_c, C_H and C_{diff} are the space charge region (SCR), inner Helmholtz plane (IHP) and outer Helmholtz plane (OHP) capacitances respectively. E_c is the electrode conduction band edge and E_F its Fermi level. Reproduced from [16].

The Helmholtz model links the IHP capacitance, C_H, to the surface area of the electrode (A) via equation 2.1:

$$C_H = k_0 \varepsilon \frac{A}{\delta_{dl}} \tag{2.1}$$

Where k_0 is the vacuum permittivity (8.85 x 10^{-12} F m^{-1}), ε is the dielectric constant of the electric double layer region, and δ_{dl} the thickness of the double layer (order of the nm).

2.1.3 Pseudocapacitors

2.1.3.1 Definition of pseudocapacitance

To improve the capacitance of electrochemical capacitors, it is possible to exploit faradaic (redox) processes at the surface of the electrodes. The processes influence the electrochemical signature of the electrode and can be studied using cyclic voltammetry and galvanostatic charge/discharge cycles (Figure 2.3a and b). The resulting electrode is defined as pseudocapacitive [17-19].

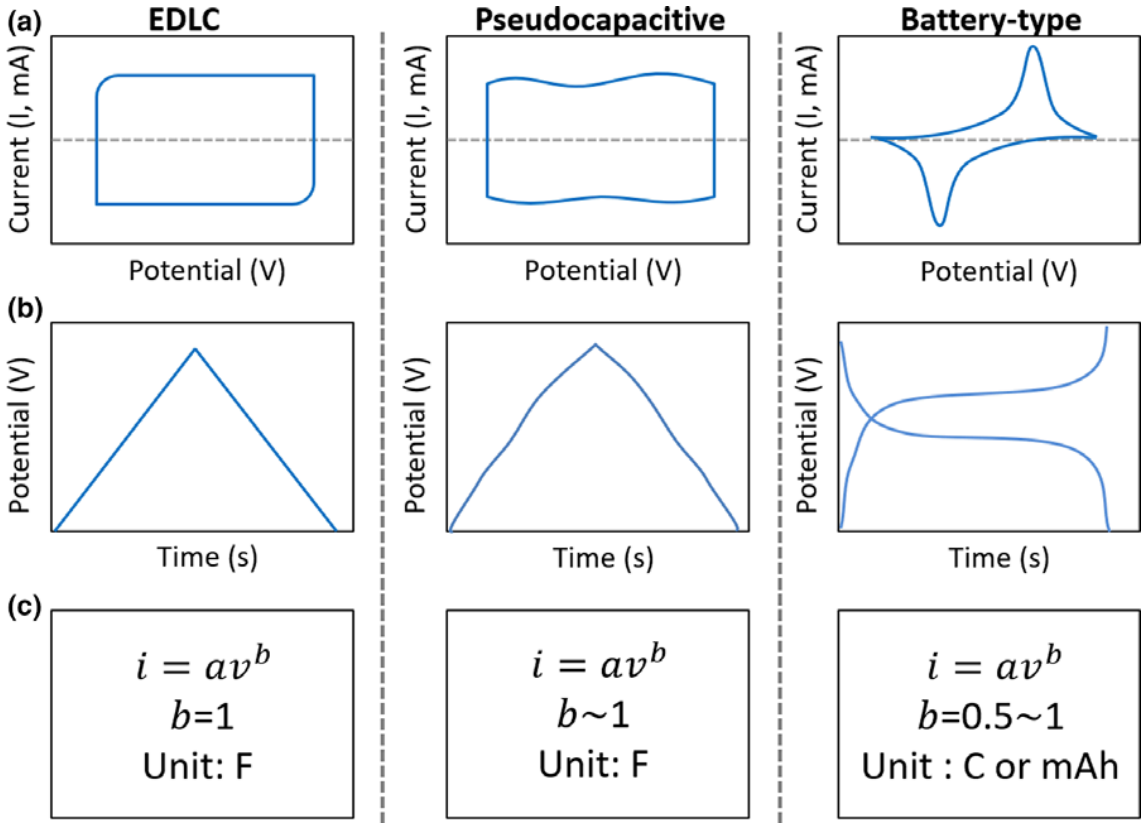

Figure 2.3 a) Cyclic voltammetry and b) galvanostatic charge/discharge curves for electrical double layer capacitors, pseudocapacitive (surface faradaic reactions) and battery-like (bulk faradaic processes) materials. c) Dependence of the peak current (i) with the scan rate (v) and correct unit to evaluate the material's charge storage performance. Reproduced from [18].

When faradaic processes are added to the electrode (via surface doping or active material deposition), the charge storage capacity enhancement can be limited by two different factors: the kinetics of the redox surface reaction or ion diffusion [18]. In the former case, the redox reactions occur at the surface of the electrode which is called pseudocapacitive and capacitance (in Farad - F) is the correct figure of merit to evaluate the charge storage capacity. In the latter, the reactions take place in the bulk of the electrode. These electrodes are called battery-type and should be evaluated by their capacity (in Coulombs – C) [18]. Figure 2.3 represents the typical cyclic voltammetry and galvanostatic charge/discharge for EDLCs, pseudocapacitive and battery-like electrodes. EDLC cyclic voltammograms feature a rectangular shape that becomes quasi-

rectangular for pseudocapacitive material due to the faradaic processes. Battery-like materials feature sharp oxidation and reduction peaks. For galvanostatic charge and discharge curves, ELDCs present a linear variation of potential with time. Again, the shape is only slightly altered for pseudocapacitive materials while battery-like electrodes feature large plateaus corresponding to bulk oxidation and reduction.

Using very high specific surface area current collectors, some battery-like electrodes can be tailored to exhibit pseudocapacitive behaviors as the bulk and the near surface portions of the redox-active material *fuse* together.

To differentiate the surface-limited pseudocapacitive materials from the diffusion-limited battery-like electrodes, the current intensity (i) of a peak in a cyclic voltammetry can be linked to the scan rate (v) by equation 2.2:

$$i \approx a v^b \tag{2.2}$$

Where a depends on the chemical reaction kinetics and b is 1 or almost 1 for EDLCs and pseudocapacitive materials and 0.5 for diffusion-limited processes (battery-like) [20, 21].

2.1.3.2 Link between capacity and capacitance

The specific capacity of an electrode or device is the maximal number of charges that can be stored per unit of mass or area. The specific capacity by mass (Q) is reported in C g^{-1} or mA h g^{-1}. As C is equivalent to A s, a simple multiplication by 3.6 allows to switch between these two units:

$$Q_{mA\ h\ g^{-1}} = 3.6\ Q_{C\ g^{-1}} \tag{2.3}$$

The capacitance is a property of the electrode or device and, contrary to capacity, does not depend on the voltage excursion. For these materials, the capacitance and capacity are linked by equation 2.4:

$$Q = C\ \Delta V \tag{2.4}$$

Where Q and C are respectively the capacity and capacitance of the device and ΔV the potential excursion.

Battery-like (or faradaic) electrodes must be characterized by their capacity as the previous equation is not verified. This is due to redox reactions occurring at defined potentials. Thus, the capacitance will not be constant throughout the potential excursion.

2.2 Tannins

2.2.1 Classification and molecular structure

2.2.1.1 Classification and common uses

Tannins are secondary plant metabolites omnipresent in the plant kingdom, second in abundance only to lignin and cellulose [22]. They are a polyphenol family regrouping over a thousand molecules of different structures and properties [9]. Nonetheless, they can be classified into two categories: hydrolyzable and condensed tannins. Hydrolyzable tannins include the gallotannins, ellagitannins and complex tannins subgroups. They are found in nature as single molecules while condensed tannins are found as oligomers of their composing tannins. Hydrolyzable tannins, such as tannic acid and pyrogallol (Figure 2.4) have molecular weights ranging between 500 and 5 000 Da, are water soluble and their extraction is simple and take place through non-toxic processes [23, 24]. Condensed tannins, such as catechin, epicatechin and epicatechin gallate (Figure 2.4) have higher molecular weight, ranging between 5 000 and 20 000 Da (in oligomer form) [25]. They are structured around the same flavan-3-ol core. Catechin and epicatechin are enantiomers. Epicatechin gallate presents the addition of gallic acid through an ester bond. Tannic acid is formed by gallic acid molecules linked together by ester bonds and centered around a D-glucose cycle. The structure of pyrogallol is a vicinal tri-phenol cycle.

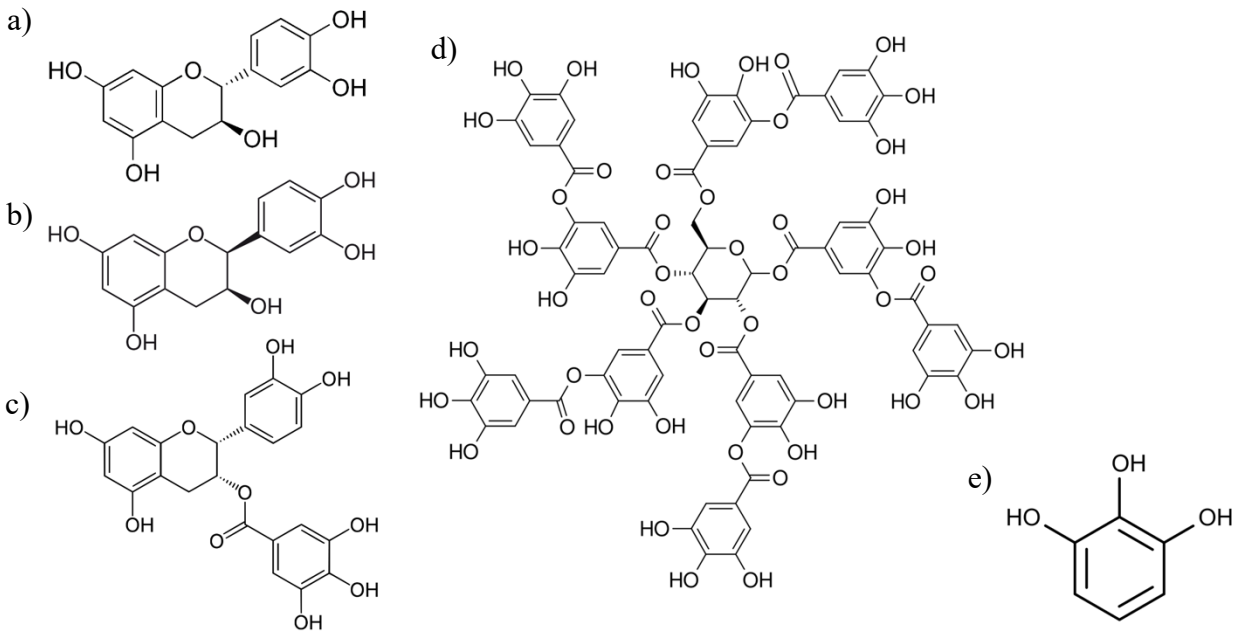

Figure 2.4 Molecular structures of the tannins investigated in this work: a) catechin, b) epicatechin, and c) epicatechin gallate, d) tannic acid and e) pyrogallol.

A simple route exploits their presence in forestry waste (12% to 16% of the weight of dry bark [22]). Dry bark is immersed in water and shaken for 8 to 10 hours at room temperature or 10 to 15 minutes in boiling water. The obtained solutions are filtered and concentrated using a rotary evaporator and a concentrated tannin powder can be obtained after drying the compound in a vacuum chamber [12, 26]. The simplicity of the extraction process is a double-edged sword as rainwater can extract tannins from abandoned forestry waste resulting in water contamination and toxicity (from their anti-oxidant properties) [12].

Tannins inherited their name from the Gaelic word “Tan” meaning oak. Oak bark was in fact the first source from which tannins were extracted and used since ca. 1 500 B.C. for leather tanning. More recently, studies focus on their antioxidant [27], antitumor [28, 29] and antiviral [30] properties for medicinal applications [31]. Finally, their reversible redox activity is starting to attract attention for electrochemical energy storage devices.

2.2.1.2 Redox-active sites

On average, tannins present the highest phenol density amongst all biosourced molecules, with phenol densities up to 5 000 higher than lignin, a molecule well known for electrochemical energy storage applications [32]. However, their great structural diversity results in variations in their electrochemical signature complicating the development of a universal application route. Therefore, other biopolymers such as lignin have been more explored for electrochemical energy storage, despite their lower redox-active site density [23].

All tannins feature the redox-active couple catechol (hydroquinone)-quinone that undergoes a two-proton, two-electron transfer (Figure 2.5) [33].

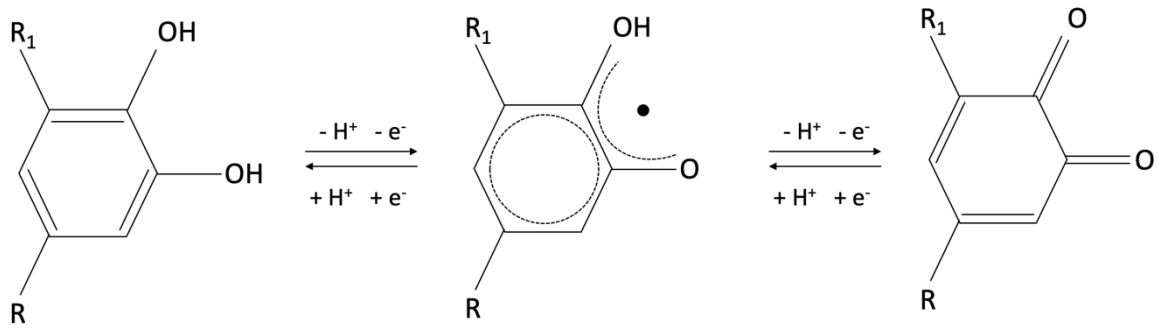

Figure 2.5 Reversible oxidation of catechol into catequinone. R is a rest that changes for different members of the tannin family whereas R_1 can be a third -OH group or simply an H.

2.2.1.3 Adhesion on carbon

Tannins are known to adsorb on carbons [7]. Tannic acid is used to stabilize carbon nanotubes (CNTs) suspensions by adsorbing on their surface e.g. through π-π interactions [34]. Lehmann *et al.* [35] studied the adsorption equilibrium of gallic acid as representative of tannin mixtures extracted from switchgrass and reported a maximum of 1.2 mmol of gallic acid (204 mg) adsorbed per gram of activated carbon. Soetaredjo *et al.* [36] used activated carbon to recover catechin and epicatechin from water contaminated by waste of the Sago tree of Papua New Guinea (e.g. bark and leaves left from the forestry industry). They found that, although enantiomers, the two tannins have very different maximal adsorption capacity on activated carbon: 74 mg g^{-1} for catechin for only 29 mg g^{-1} for epicatechin.

2.2.2 Tannins for electrochemical energy storage

Tannins have recently started to attract attention for electrochemical energy storage [23, 33].

2.2.2.1 Tannins as binders

Strong and durable metal-phenol bonds have been used to promote the cycling stability and mechanical strength of Fe^{3+}/tannic acid electrodes [37]. The hydrogen-bonding properties of tannic acid were used to improve the stability of silicon anodes in lithium-ion batteries [38]. The mechanical strength of reduced graphene oxide (r-GO) or CNTs electrodes was also improved using tannic acid to fabricate flexible electrochemical capacitors [39, 40].

2.2.2.2 Tannin as carbon precursors

Tannins have also been used as precursors for carbonization. The resulting carbon electrodes contain numerous oxygen functionalities, have high specific surface area and achieve high capacitances [41, 42].

2.2.2.3 Tannins as redox-active material

Finally, tannins have also been investigated as biosourced redox-active materials. Tannic acid has been used in electrochemical capacitors [39] and cathodes for lithium-ion batteries [43] with the role of binder for small silicon particles or even as the active redox material. Lemieux *et al.* [44] studied the intrinsic charge storage properties of tannins (tannic acid and catechin) on carbon paper electrodes and achieve areal capacity of about 2.4 x 10^{-4} mA h cm^{-2} for both molecules. Gouda *et al.* [8] continued this study by interfacing the tannins on newly modified carbon paper to reach 300 F g^{-1} specific capacitance for catechin/tannic acid (where tannic acid was added to act as binder).

Mukhopadhyay *et al.* [23] associated tannins and polypyrrole (a conductive polymer) to achieve even higher capacitances. Tannins, extracted directly extracted from bark, are deposited onto polypyrrole coated electrodes. They reported a capacitance increase from 94 to 370 F g^{-1} at 0.5 A g^{-1} on gold current collector. When cycled between 0.05 and 3.3 V a lithiated ellagic acid electrode delivered capacities of 450 and 200 mA h g^{-1} at C/10 and C/2.5 discharge rates, respectively [45]. The C-rate (in h^{-1}) is the ratio between the current density used to cycle the device and the current

required to fully charge or discharge it in 1 h. C/10 and C/2.5 indicate currents required to fully charge or discharge the device in 6 and 24 min respectively.

2.3 Surface properties of electroactive carbons: surface area and chemistry

2.3.1 Fundamentals on electroactive carbons and capacitance

Carbon has attracted a lot of interest because of its different crystalline allotropes (diamond – sp^3, graphite – sp^2, carbene – sp^1 and fullerenes – "distorted" sp^2), the possibility to easily change its microtexture (unit cell structure) and a wide range of dimensionalities (powders, 1D carbon nanotubes, 2D graphene sheets and 3D carbon aerogels) [19, 46] [47]. These parameters allow to create countless forms of carbon materials with different properties [48]. Other interesting properties of carbon materials are the strength of the C-C covalent bond, making for durable materials, and the surface chemistry that is compatible with organic and inorganic surface depositions [49]. Some carbon-based materials present interesting properties for electrochemical energy storage such as, high specific surface area and controlled pore structure, mechanical stability, polarizability, electrical conductivity, chemical stability and low cost [19, 46].

Literature reports examples of electrochemical capacitors using several different carbon-materials such as activated carbons [50-52], carbon fibers [53-55], carbon nanotubes (CNTs) [56-59], graphene [60-62] and graphene quantum dots (GQDs) [63]. GQDs are edge-bound nanometer-sized graphene structures that make use of quantum confinement to tune electrical and optical properties. Nann's group reported on the properties and creation methods of GQDs [63]. GQDs are traditionally obtained through expensive, long, and low yielding methods such as electron-beam lithography or metal-catalysed C_{60} transformation processes. Recent efforts have shown that simple acid treatments can create GQDs on the surface of carbon fibers [64, 65].

2.3.2 Importance of the specific surface area and pore structure

Carbon-materials can have very high specific surface area, ranging from 200 to over 3 500 $m^2\ g^{-1}$ [50, 51] and high pore volume from 0.4 to over 1.6 $cm^3\ g^{-1}$ [19, 50]. However, increased specific surface area is not directly linked to higher capacitance, as shown in table 2.1. This can be explained by considering that the specific surface area is measured by using the Brunauer, Emmett and Teller (BET) method making use of dinitrogen gas molecules. These molecules are often much smaller than electrolyte ions and their gaseous state neglects intermolecular interactions that can arise in liquid phase.

Table 2.1 Comparison of specific surface areas and capacitance for different activated carbons found in literature. Reproduced from [2].

Carbon	Specific Surface Area ($m^2\ g^{-1}$)	Specific Capacity ($F\ g^{-1}$)
M-10	1370	55.95
M-14	1223	57.2
M-15A	1800	78.1
M-15B	1624	55.8
M-15C	1518	63.34
M-20	2130	100
M-30	2571	62.9
A-10	1150	35.3
A-20	2012	41.2
SACF-20	1839	48.8
SACF-25	2371	27.9

IUPAC categorises pores into three groups depending on diameter size: micropores (less than 2 nm), mesopores (between 2 and 50 nm) and macropores (greater than 50 nm) [47]. Micropores have the higher surface to volume ratio and microporous materials can achieve great surface areas but that are mostly inaccessible and not contributing to the device capacity [19, 46]. Thus, before choosing the carbon electrode material, an investigation into pore size distribution is often required in addition to surface area measurements.

2.3.3 Techniques to activate carbon

Carbon activation is a simple, low cost and efficient method to increase specific capacity.

Carbon activation is a controlled oxidation of the surface to open inaccessible pores (either closed of clogged) in order to increase the surface area and consequently the ion electrolyte-accessible surface area [50]. Several activation techniques are known: thermal, chemical and electrical activation [46, 54] [66].

Thermal activation is carried out by oxidising gases (air, carbon dioxide, steam, or their mixtures) at temperatures between 1000 and 1400 K. The choice of temperature, oxidising gas and treatment duration allow to control the activation process [46].

Chemical activation uses oxidising agents such as sulfuric or nitric acid [53, 64] and potassium hydroxide [55] to remove residues (organic or inorganic) from the carbon precursor, thus, “cleaning” the pores and increasing accessibility. Chemical activation, through potassium hydroxide, can achieve specific surface areas above 2500 m^2 g^{-1} [46, 55]. By using mixtures of sulfuric and nitric acids, Hsiao *et al.* [64] enhanced surface area of carbon fibers and created GQDs on the surface.

Electrical activation is carried out by applying galvanostatic anodic current or potential to the electrode material. This method has shown to increase surface area and increase capacity by one order of magnitude for polymer-coated carbon electrodes [54, 67].

2.3.4 The influence of surface chemistry

Surface chemistry has a great influence on the capacitance [49]. The termination of the bulk carbon structure is atomically ordered and formed of strong carbon-carbon bonds with however naturally occurring oxygen-groups due to air-oxidation. Tailored surface treatments can allow to choose the concentration and oxidation level of such groups greatly influencing wettability, by creating dipole-dipole interactions with the aqueous solvent [49]. Wettability impacts the access of ions to the carbon surface [68].

Surface functionalization is not the only surface treatment that can enhance efficiency of the electrode and improve the capacitance. "Click chemistry" allows to create layer by layer polymer growth on the surface of carbon structures [68, 69]. Finally, using diazonium derivates, McCreery's group was able to grow graphene ribbons on the surface of the carbon structure to create a graphene "brush" 2 to 20 nm-thick [70, 71]. This "brush" brought about energy density beyond 10 Wh kg^{-1}, values closer to lithium-ion batteries than commercially available carbon electrochemical capacitors [72]. By introducing Faradaic processes, through the addition of redox-active nitrogen-groups, McCreery *et al.* achieved record capacitances [73].

2.3.5 Examples of electroactive carbons

Now that the general properties of electroactive carbons have been explored, let us review a few examples of such technologies.

2.3.5.1 Carbon fibers

Carbon fibers are one dimensional (diameter ca. 10 μm) structures synthetized through thermosetting organic precursors such as cellulose or polyacrylonitrile at temperatures from 1 100 to 1 800 K [46]. The nature of the precursor and the surface treatment have a great impact on the quality of the fiber (surface area, conductivity, mechanical resistance). Carbon fibers are predominantly microporous but, owing to their small dimension, pores are predominantly on the surface and a simple oxidizing treatment allows to control surface area (specific surface area up to 2300 $m^2\ g^{-1}$ are reported [55]) and pore distribution making activated carbon fibers very interesting

for electrochemical capacitor applications [46]. The electrochemical storage performance of carbon fiber electrodes can be further improved using redox active coatings such as polyaniline [54] or melanin [74].

Surface investigation of carbon fiber through x-ray photoelectron spectroscopy (XPS) shows a predominant carbon surface (over 90%) with the possibility to increase oxygen functional groups (hydroxyl -OH, carbonyl -C=O, and carboxyl -COOH) up to 18 % oxygen content through oxidising treatment. The rest of the surface elements are composed of 2% nitrogen (regardless of the oxidation treatment time) and traces of various elements that have no impact on the surface reactions [53]. Figure 2.7 shows the parallel role of sulfuric and nitric acid in the chemical activation of carbon fibers: nitric acid adds more nitrogen functionalization while sulfuric acid creates rougher surfaces by etching of carbon fibers [64]. It is important to keep in mind that XPS investigation focuses only on the first layer (ca. 10 nm in depth) and that the bulk material is still composed only of carbon even after extensive oxidation treatment [75].

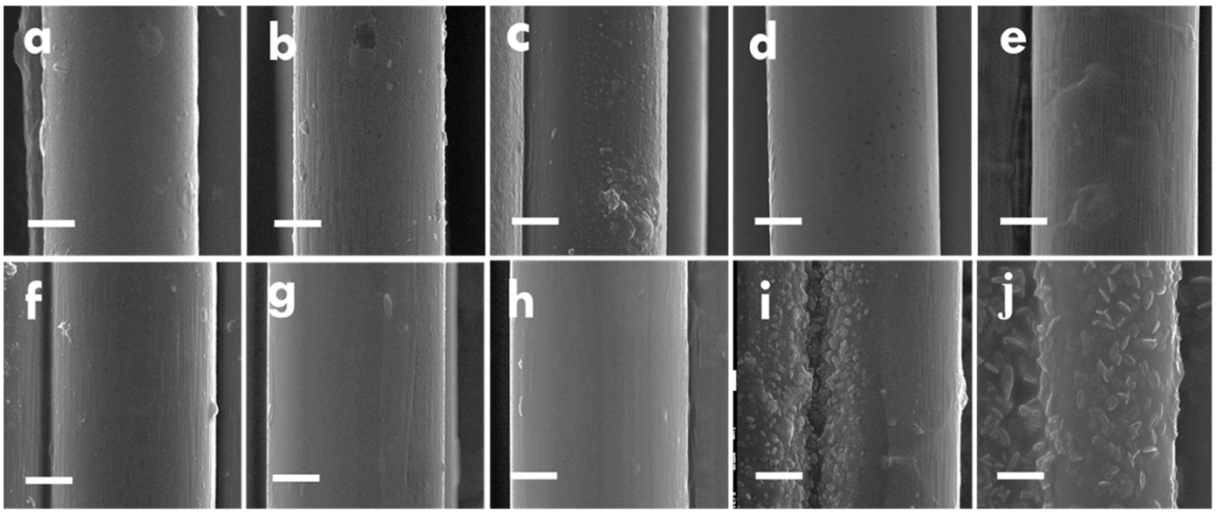

Figure 2.6 Scanning electron microscopy of a) untreated carbon fiber and different proportions of sulfuric and nitric acid: b) only nitric acid, c) 4:1 nitric-sulfurid acids, d) 2:1 nitric-sulfurid acids, e) 1:1 nitric-sulfurid acids, f) 1:2 nitric-sulfurid acids, g) 1:3 nitric-sulfurid acids, h) 1:4 nitric-sulfurid acids, i) 1:5 nitric-sulfurid acids, j) only sulfuric acid. Reproduced from [64].

2.3.5.2 Carbon nanotubes

Carbon nanotubes are one atom-thick sp^2 carbon structures "rolled-up" to form tubes of nanometer-scale diameters [76]. CNTs have attracted great attention due to their high stability (chemical and mechanical), conductivity and electrochemical properties [66]. They can be organised into two categories: single and multi-walled carbon nanotubes (SWCNTs and MWCNTs) depending on the number of rounds completed by the structure. SWCNTs have a theoretical surface area as high as 1315 $m^2\ g^{-1}$ before any oxidation treatment [59]. However, experimentally measured surface areas are found to be between 200 and 400 $m^2\ g^{-1}$ [56, 57] due to two main factors. The former factor, MWCNTs present decreasing theoretical specific surface area with the increase of the number of walls: theoretical surfaces of 680 to 850 $m^2\ g^{-1}$ for 2-walled CNTs and 295 to 430 $m^2\ g^{-1}$ for 5-walled CNTs [59]. The latter factor that contributes to decreasing surface area is the presence of bundles of CNTs blocking the access to part of the surface. Futaba *et al.* [58] showed that controlled growth of CNTs into highly densely packed, vertically aligned SWCNTs can achieve 1 000 $m^2\ g^{-1}$ specific surface area while maintaining conductivity and flexibility.

CNTs can also be activated through oxidising treatment resulting in an improvement of specific surface area by a factor of 2 to 5 without altering the diameter of the tubes. However, the oxidation treatment is reported to shorten the length of the tube by creating large, easily accessible distortions in the carbon structure [46, 51, 66]. Previously presented activation treatments on CNTs can achieve up to 20% surface oxygen by number of atoms and 2% nitrogen incorporated with the same functional groups as carbon fibers.

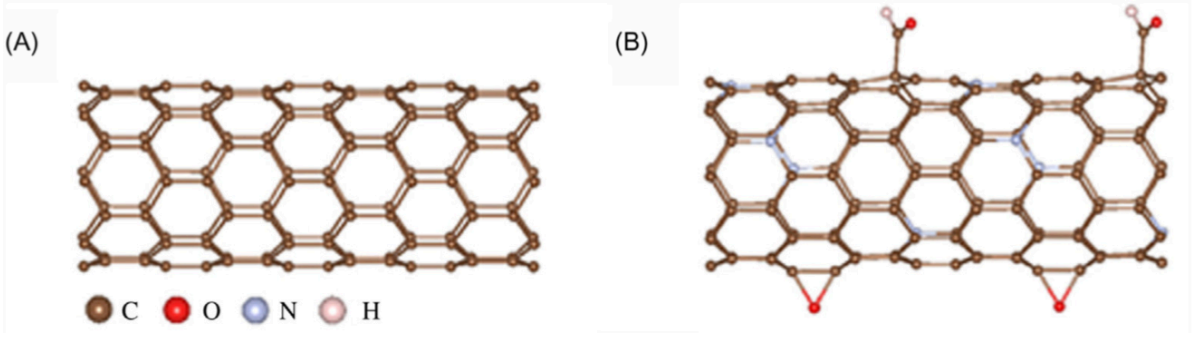

Figure 2.7 Structure of single-walled carbon nanotube A) before and B) after oxidising treatment by potassium hydroxide and nitrogen doping. Reproduced from [66].

2.3.5.3 Graphene

Graphene is a 2-dimensional planar sp^2 allotrope of carbon that can be synthesised or derived from natural graphite [46, 66, 77]. Graphene sheets are planar, one atom thick and composed of σ (single bond) carbon atoms disposed in a regular honeycomb lattice. Scanning electron microscopy (SEM) images show a very flat surface with rough leaf-like shapes on the surface corresponding to stacked sheets [77]. Natural graphite is an extremely pure form of carbon, presenting less than 1% of heteroatoms on its surface via XPS analysis [77] and a very high theoretical surface area of up to 2600 $m^2\ g^{-1}$ [51, 61]. Therefore graphene-based electrochemical capacitors are extensively studied for flexible and transparent electronics [51, 66]. However, BET-measured specific surface area is reported to be much lower (300 to 700 $m^2\ g^{-1}$ [60-62]) due to stacking of graphene sheets and poor wettability. Functionalization into graphene oxide can increase surface oxygen to 20–40% by atomic concentration improving wettability and reducing stacking [77]. Furthermore, conducting polymer coatings and metal sheets can be intercalated between graphene sheets to create pseudocapacitance effects thus device capacity [61, 66].

2.3.5.4 Other dimensionalities for electroactive carbons

Other examples of diverse dimensionality of carbon structures are 0 and 3-D structures: carbon black and carbon aerogels.

Carbon blacks are pure carbon powders produced by thermal decomposition or partial combustion of hydrocarbons in gas phase. Carbon blacks can vary in quality (fineness, aggregation, surface properties) depending on the manufacturing process. They present specific surface area from about 10 to 1 500 $m^2\ g^{-1}$ and are used as conductive fillers for other electrodes materials [46].

Carbon aerogels are prepared by pyrolysis of organic gels. By changing the organic precursors and the pyrolysis parameters, the pores density and shape can be controlled allowing to create carbon structure with high surface areas (400 to 1 000 $m^2\ g^{-1}$) and uniform mesopore distribution (2 to 50 nm). Finally, surface area can be further increased (up to 2 000 $m^2\ g^{-1}$) by oxidative treatments [46].

CHAPTER 3 EXPERIMENTAL

3.1 Investigation methods

3.1.1 Scanning electron microscopy

Scanning electron microscopy (SEM) was used to analyze the surface morphology of the electrodes with and without tannins. SEM measures the interactions of a focused electron beam with the surface of a sample to characterize its morphology. The surface topography can be reconstituted using an Everhart-Thornley detector to collect secondary electrons. These electrons are emitted from surface atoms following the excitation caused by the absorption of an electron from the main beam [78]. In this work, we use silver staining to detect the tannins on the surface of the carbon and make use of backscattered electrons to observe the morphology of the silver. Backscattered electrons are electrons reflected by surface atoms without being absorbed. Large atomic number atoms (like silver) reflect electrons more than low atomic number atoms (like carbon) allowing us to observe the difference in chemical structure of the surface [78].

The staining of tannins using silver nitrate ($AgNO_3$ – ACS reagent > 99%) is based on the reduction properties of tannins on metallic cations [79]. To stain the samples, a simple immersion in a 0.1M silver nitrate solution for 48h was sufficient. The electrodes were rinsed and dried under vacuum before entering the SEM chamber.

3.1.1.1 Morphological experiments

We studied the surface morphology of carbon paper, treated carbon paper and carbon paper with tannins using scanning electron microscopy (SEM, JEOL JSM7600F) at an acceleration voltage of 5 kV. To reveal the tannins on the carbon paper, we stained the samples by immersing them in a silver nitrate (0.1 M $AgNO_3$ – ACS reagent > 99%) solution for 48 h [79]. Samples were rinsed in deionized water and dried under vacuum for 30 min at 60 °C before entering the SEM chamber. To identify the different elements on the surface of the carbon, we performed energy dispersive X-ray spectroscopy (EDX) using the same scanning electron microscope with Aztec (Oxford) software, detector x-Max (80 mm^2) (Oxford), at 5 kV.

3.1.2 X-ray photoelectron spectroscopy

XPS is a quantitative spectroscopic technique used to characterize the chemical composition of the surface of a material. It is based on the photoelectric effect, that is the emission of an electron upon electromagnetic excitation of the material, in this case through X-ray radiation [80]. The three main components of an XPS instrument are: an X-ray source, an extraction optic and energy system, and a detection system. Furthermore, the environment inside the instrument must be precisely controlled. No electrostatic or magnetic fields must perturbate the emitted electrons. An ultra-high vacuum (typically below 10^{-9} mbar) must be kept at all times so that the mean free path of the emitted electron is greater than the distance between the sample and the detector [81].

By measuring the kinetic energy of the emitted electrons, XPS gives insight on the atomic composition of the surface of the sample. XPS provides precise information about the electronic properties of the surface atoms and allows, in part, to determine the most common interatomic bonds [80].

3.1.2.1 Surface chemistry experiments

In this work, XPS experiments were conducted using a VG ESCALAB 2250 X-ray spectrometer. The elemental composition of the untreated carbon paper, the treated carbon paper and the tannin-on-carbon electrodes was determined using an Al Kα (1486.6 eV) X-ray source at a power of 1 W (1 kV, 1 mA) under ultra-high vacuum (below 10^{-9} mbar).

The elemental composition of the surface was carried out using scans of 1.0 eV energy steps. For each element, high resolution scans (0.1 eV energy steps) were conducted to obtain more precise information.

3.1.3 Brunauer-Emmett-Teller method

The BET method was developed by Stephen Brunauer, Paul Emmett and Hugh Teller in 1938 and allows to measure the specific surface area of a porous material using the physical adsorption of gas molecules on the solid surface [82]. N_2 is the most used gas adsorbate for this method because it is non-reactive, relatively small (about 3.6 Å – allowing it to access the entire surface), and low

cost. Therefore, BET is usually conducted at the boiling temperature of N_2 (-196 ˚C). Other adsorbates can be used if a different temperature is required [83].

BET theory is based and extends Langmuir's theory on molecular adsorption. The measurement is carried out by increasing then decreasing the pressure in the chamber and observing the Langmuir isotherm of the sample. The variation of the pressure with the quantity of adsorbate gas inserted in the chamber gives insight on the specific surface area of the material and its pore distribution [84].

3.1.3.1 Surface area measurements

The BET surface area, pore volume and pore size were measured for untreated and treated carbon paper using N_2 adsorption and desorption isotherms (Micromeritics, model TriStar 3000). To prepare for the measurement, samples were degassed under vacuum overnight at 120℃. The analysis was carried out at -196 ˚C using N_2 as a gas adsorbate.

3.1.4 Electrochemical characterization

Several techniques can be used to evaluate the electrochemical performance of electrochemical capacitors, the most used being cyclic voltammetry (CV), electrochemical impedance spectroscopy (EIS) and galvanostatic charge/discharge (GCD).

3.1.4.1 General setup

The three techniques mentioned above can be conducted using the same experimental setup (electrochemical cell and potentiostat equipped with an impedance module).

The electrochemical cell is composed of three electrodes (working, counter and reference), an electrolyte to ensure ion conductivity and close the circuit in a container. The working electrode is the focus of the experiment, the counter serves to close the circuit and the reference electrode is used to measure potential differences. In this work we use 0.5M sodium sulfate in water as the electrolyte to work at near neutral pH (about 6). A glass cell and Teflon cap are used to contain the electrodes and electrolyte and nitrogen is used to degas the oxygen in solution [85].

To study a single electrode, we used it as working electrode, platinum mesh was the counter and Ag/AgCl (3M NaCl) as reference (Figure 3.1). For the catechin/tannic acid symmetric electrochemical capacitor, the two tannins-on-carbon electrodes were used as working and counter.

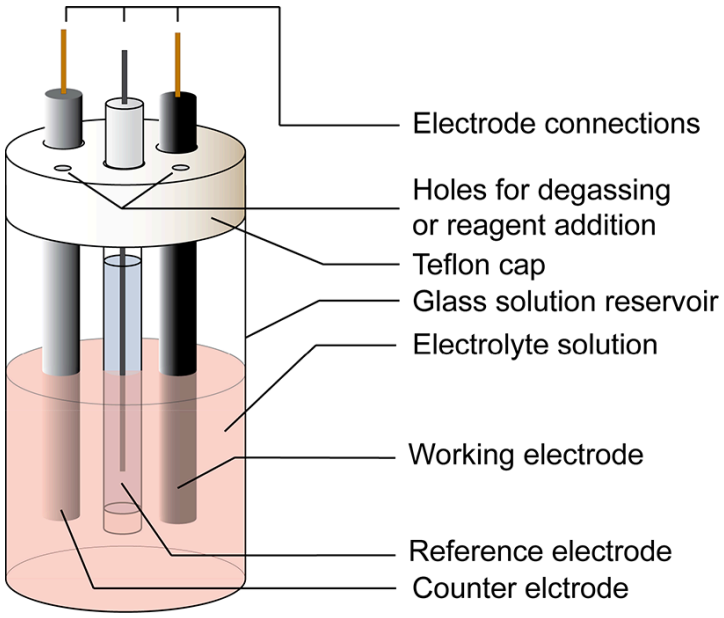

Figure 3.1 Scheme of an electrochemical cell in a three-electrode setup. Reproduced from [40].

3.1.4.2 Cyclic voltammetry (CV)

During a CV experiment, we measure the current response of the working electrode to a potential bias between it and the reference electrode. To that end, a varying (at a certain scan rate) potential difference is applied between the working and reference electrode and the current response is measured.

By observing the shape of the current versus potential curve, we can have an insight into the electrochemical processes of the electrode. Standard electrochemical capacitors present a quasi-rectangular shape indicating electrostatic processes, while faradaic reactions present in electrochemical capacitors are reflected in significant current peaks at certain potentials (Figure 3.2).

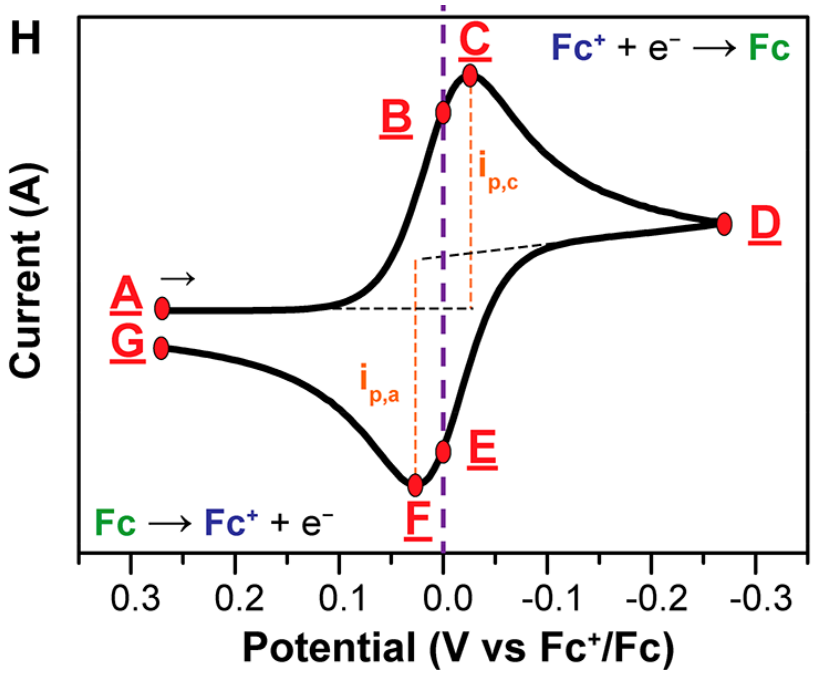

Figure 3.2 Scheme of a cyclic voltammetry scan for a pseudocapacitive electrode presenting redox activity. A – Starting potential for the scan, B and E – Standard redox potential (Nernst potential) of the considered molecule, C – Oxidation peak, D – Switch potential, F – Reduction peak, G – End of the scan. Reproduced from [85].

Furthermore, CV scans grant access to the specific capacity, Q_{CV}, (in C g^{-1} or C cm^{-2}) of the electrode using equation 3.1:

$$Q_{CV} = \int \frac{IdV}{\nu\,\pi} \tag{3.1}$$

Where $\int IdV$ is the integral area of the CV discharge, ν the scan rate, π the mass loading of the active material on the current collector or the footprint area.

Using equation 2.4, for capacitive or pseudocapacitive electrodes, we can calculate the specific capacitance, C_{CV}, (in F g^{-1} or F cm^{-2}) from equation 3.2:

$$C_{CV} = \int \frac{IdV}{\nu \, \pi \, \Delta V} \tag{3.2}$$

Where ΔV is the potential range.

3.1.4.3 Electrochemical impedance spectroscopy (EIS)

EIS measurements use alternative currents or potentials of different frequencies to measure the complex impedance of the equivalent circuit created by the electrode. The results are usually presented as Nyquist plots: the negative of the imaginary part of the complex impedance versus the real part (Figure 3.3). The interpretation of these plots can grant access to the electrode resistance (higher frequencies), the electrolyte resistance and the diffuse layer resistance as well as the capacitance (lower frequencies) [86].

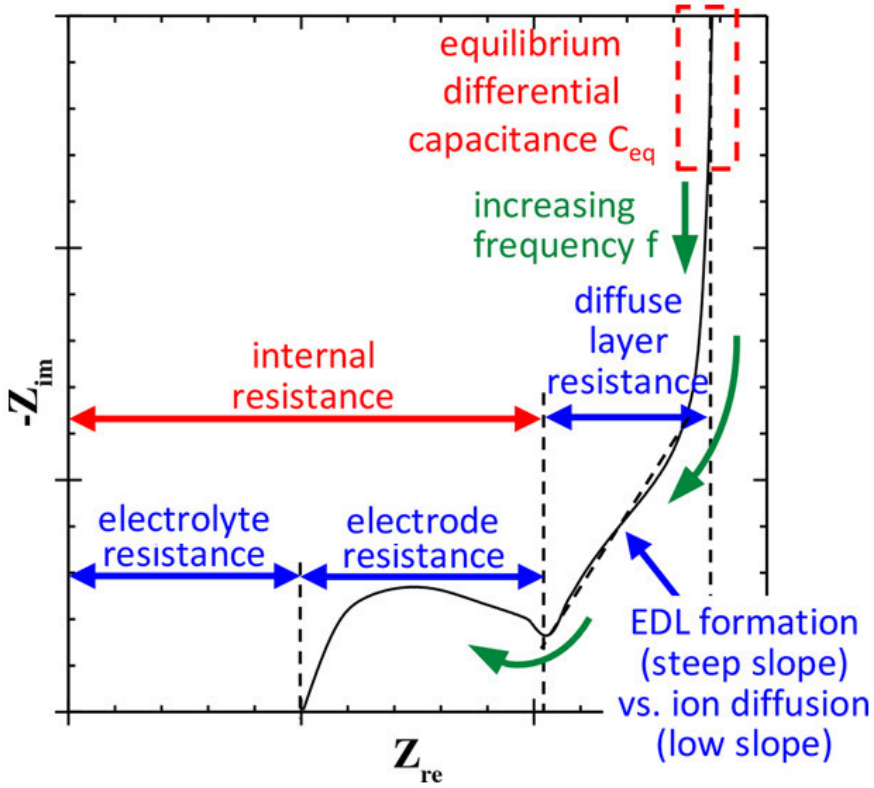

Figure 3.3 Standard Nyquist plot for an electrical double layer capacitor presenting the different information that can be extracted from the experiment. Reproduced from [86].

3.1.4.4 Galvanostatic charge and discharge (GCD)

During GCD, a constant current is applied between the working and the counter electrode, and the potential difference is measured. During the charging phase, the current is applied from the counter to the working electrode causing the potential to increase until a cut-off threshold is reached. The current is then inverted until the potential decreases to the lower switching potential.

GCD results are often presented as a plot of the potential response over time (Figure 3.4). Electrical double layer capacitors present a characteristic triangular shape, and, if present, faradaic processes of electrochemical capacitors induce slight deviations from it. A potential drop is present at the start of the discharge and can be linked using Ohm's law to the equivalent series resistance using equation 3.3:

$$\mathrm{ESR} = \frac{V_{drop}}{2\ \mathrm{I_{dis}}} \tag{3.3}$$

Where $\mathrm{I_{dis}}$ is the constant discharge current and V_{drop} the potential drop.

GCD experiments also allow to evaluate the specific capacity, $\mathrm{Q_{GCD}}$, (in C g^{-1} or C cm^{-2}) using equation 3.4:

$$\mathrm{Q_{GCD}} = \frac{\mathrm{I_{dis}}\ \Delta t}{\pi} \tag{3.4}$$

Where Δt is the discharge time and π the footprint area or the mass loading of the active material on the current collector.

Again, for capacitive or pseudocapacitive electrodes, we can calculate the specific capacitance, $\mathrm{C_{GCD}}$, (in F g^{-1} or F cm^{-2}) from equation 3.5:

$$\mathrm{C_{GCD}} = \frac{\mathrm{I_{dis}}\ \Delta t}{\pi\ \Delta \mathrm{V}} \tag{3.5}$$

Where ΔV is the potential excursion.

Equation 3.5 is equivalent to equation 3.6:

$$C_{GCD} = \frac{I_{dis}}{\pi\,\delta} \tag{3.6}$$

Where δ is the slope of the cell voltage over time during discharge.

Furthermore, the Coulombic efficiency (η), can be evaluated using equation 3.7:

$$\eta = \frac{I_{dis}t_{dis}}{I_{ch}t_{ch}} \tag{3.7}$$

Where I_{ch} is the constant charge current, and t_{dis} and $t_{ch}$the discharging and charging times.

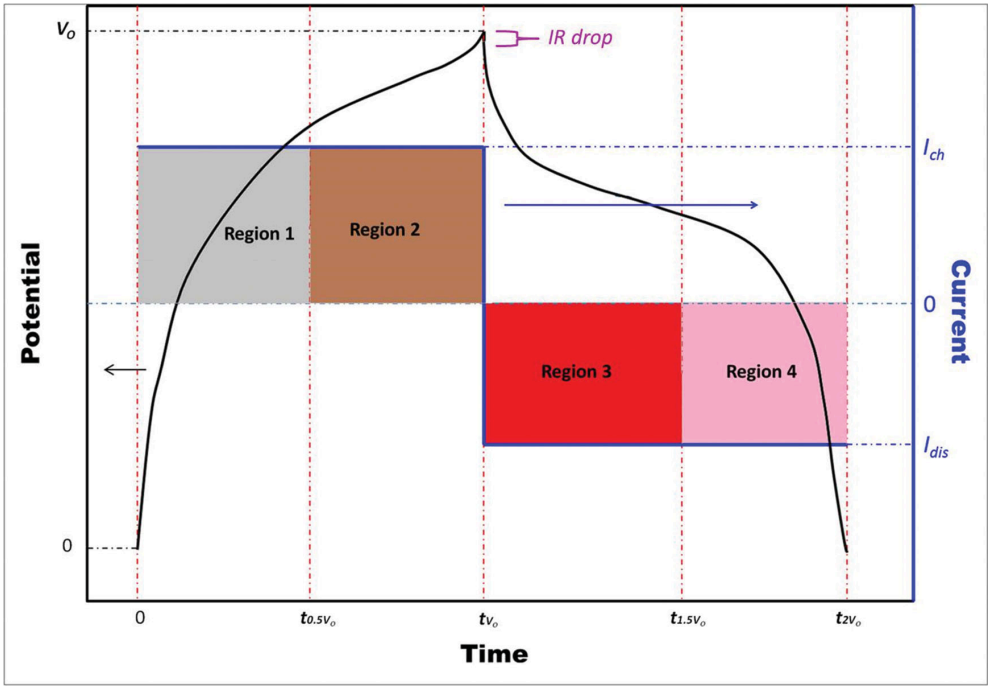

Figure 3.4 Standard galvanostatic charge/discharge plot for a pseudocapacitive material. The slopes from regions 1 and 4 give access to the capacitance of the electrode or electrochemical capacitor using equation 3, while the plateaus of regions 2 and 3 are due to the redox reaction of the active material. The IR drop (or voltage drop) is due to losses caused by the equivalent series resistance. Reproduced from [87].

The energy (E) and power (P) densities can be extracted from these plots using equations 3.8 and 3.9 respectively:

$$E = \frac{I_{dis} \int V dt}{3600} \tag{3.8}$$

$$\mathrm{P} = \frac{E}{\mathrm{t}_{dis}} \tag{3.9}$$

Finally, the maximal energy and power densities can also be extracted from these plots using:

$$\mathrm{E_{max}} = \frac{{}^{1}/_{2}\, \mathrm{C_{GCD}} \mathrm{V_{max}^2}}{3600\ \pi} \tag{3.10}$$

$$\mathrm{P_{max}} = \frac{\mathrm{V_{max}^2}}{4\ \mathrm{ESR}\ \pi} \tag{3.11}$$

Where $\mathrm{V_{max}}$ is the upper limit of the potential while charging (operating voltage or cutoff potential).

By adapting the current density, the duration of the charge and discharge cycles can be tuned. Electrochemical capacitors are known for their high-power density that allows to reach high current densities with little performance loss (good rate capability). Thus, high current density GCD experiments allow to measure the capacitance over a great number of cycles (well over 1 000) to evaluate the cycling stability.

3.1.4.5 Electrochemical experiments

We conducted CV, EIS and GCD using a Biologic bipotentiostat (SP-300).

All 5 tannins (catechin, pyrogallol, tannic acid, epicatechin and epicatechin gallate) were studied individually on carbon and treated carbon in a three-electrode configuration. The tannins deposited on the carbon electrode served as working electrode, a platinum mesh as counter and an Ag/AgCl (3 M NaCl) electrode as reference.

Catechin was chosen for further investigation in aqueous symmetric electrochemical capacitor configuration: a tannin on carbon electrode as working, another as counter, the two separated by a filter paper. Tannic acid was used as a binder giving a catechin/tannic acid symmetric electrochemical capacitor. The proportion of catechin to tannic acid used as binder was 7:1 (w:w)

We used 0.5 M Na_2SO_4 as electrolyte for all aqueous measurements (pH about 6).

For all electrodes, we first measured the open-circuit voltage for 5 min. Then, we conducted EIS measurements at open circuit potential, before and after the CV, at 10 mV alternative potential amplitude and within the frequency range of 10^5 to 10^{-1} Hz. For CV, we scanned the potential from -1 to 1V vs. Ag/AgCl, at scan rates of 100, 50, 20, 10 and 5 mV s^{-1}. For the catechin/tannic acid-based electrochemical capacitor the same scan rates and frequency range were used, and the cell voltage was 2V.

We proceeded to GCD measurements for the electrochemical capacitor device, using a reduced cell voltage of 1.6V to prevent damage to the electrodes after several charge and discharge cycles. Current densities of 0.5, 2, 4, 8, and 10 A g^{-1} were chosen to investigate the device. Using this last current density (10 A g^{-1}), we tested the stability of our devices for 5 000 charge/discharge cycles.

The active footprint area is of 0.5 cm^2 per electrode, giving 1 cm^2 for the devices corresponding to 3.0 ± 0.4 mg of tannins and 4.2 ± 0.2 mg when adding the weight of the carbon substrate.

3.2 Tannin deposition, electrodes and devices fabrication, and characterization

3.2.1 Carbon electrode preparation

Carbon paper was purchased from Fuel Cell Store (Spectracarb 2050A-1550, 10 mils, plane electrical resistivity of 5.4 mΩ cm). It is composed of multiple plies of graphitized resin-bonded carbon fibers. We applied a three-step treatment to optimize its conductivity, surface area and wettability for our study according to Gouda *et al.* [8].

The first step of the process consists of cleaning the carbon electrodes (rectangles 0.5 cm by 5 cm) to eliminate impurities. For that, we used a sequential sonication (application of sonic – or ultrasonic – vibrations to the solvent, leading to the liberation of surface impurities) in ethanol (Commercial Alcohols, Ontario, Canada) and acetone (Honeywell, VLSI, 100%), 10 minutes each at 40 kHz.

The second step consists in immerging and sonicating for 2 h (at 40 kHz) the carbon electrodes in 40 mL of acidic solution. We used a 3:1 mixture of sulfuric (H_2SO_4 – Sigma-Aldrich ACS reagents 95% - 98%) and nitric (HNO_3 – 16M Fischer Chemical, ACS plus) acids. Sulfuric acid is responsible for the increase in surface area as it etches the surface of the carbon fibers, leading to the formation of grooves and the creation of pathways to render some micropores more accessible [64]. Nitric acid induces surface functionalization which improves the wettability to aqueous (polar) solvents by adding polarized bonds at the surface of the fibers [64]. Both improve the capacitance of the bare carbon electrode: sulfuric acid by increasing the surface area, thus the electrical double layer capacitance, nitric acid, by adding redox active sites and increasing the pseudocapacitance. This solution containing the electrodes is then transferred in an autoclave for a thermal treatment of 20 min at 120 °C and a slow cool down overnight in the autoclave. The slow cool down prevents damage to the electrodes. Electrodes were rinsed before applying the third step of the treatment.

The third and final step of the treatment is similar to the second: by immersing the electrodes in a saturated solution of ammonium phosphate (7M $(NH_4)_2HPO_4$ Sigma-Aldrich, ACS reagents >

98%) and proceeding to a second thermal activation: 24h at 180 °C and overnight cool down, we added P doping to the previous O, N and S co-doping [8].

Electrodes were then rinsed with deionized water, and dried 6h under vacuum.

3.2.2 Preparation of the tannin solutions

Catechin, pyrogallol, tannic acid, epicatechin and epicatechin gallate (ACS reagents > 98%) were used as received. To deposit the active tannin materials on the surface of the carbon paper we exploited their aqueous solubility. We used a water:ethanol 2:1 mixture to prepare 40 g L^{-1} solutions of tannins.

Tannic acid was also used as a hydrogen-bonding binder for catechin [38]. Catechin/tannic acid solutions were prepared in the same fashion as single-tannin solutions presented above using a 7:1 weight ratio between the catechin and tannic acid. The addition of tannic acid did not alter the redox properties of catechin.

Using a micropipette, the desired amount was drop-casted on a 1 cm by 0.5 cm surface of the carbon. We then vacuum dried the tannin-on-carbon electrodes for 30 min at 60 °C. For all tannins, the mass loading was 0.3 ± 0.1 mg and 1.5 ± 0.2 mg on 0.5 cm^2 of untreated and treated carbon, respectively (evaluated using a Sartorius BP 210 D microbalance of accuracy 10^{-5} g).

CHAPTER 4 ELECTROCHEMICAL PROPERTIES OF TANNINS ON CARBON ELECTRODES

4.1 Effect of the carbon treatment

To improve the tannin/carbon interface and the charge storage performance of the tannin-on-carbon electrodes, we used a chemical (oxidative) and thermal treatment of the carbon paper. Such acid-based chemical and thermal treatments are well known in literature and have been shown to improve several properties of the carbon fibers (e.g. surface area, surface doping, and conductivity through the formation of graphene quantum dots) [64, 65]. The activation protocol used in this work is based on the work by Hsiao *et al.* [64] that compares the optimal proportions between sulfuric and nitric acids. This work was improved by Gouda *et al.* [8] to add P surface doping.

4.1.1 Specific surface area enhancement

The use of sulfuric acid is responsible for etching of the fibers, resulting in an increase in specific surface area due to the increase in the roughness of the fibers and larger accessibility of micro and mesopores (Figure 2.6) [64]. The pore volume and surface area measurements were performed using N_2 adsorption and desorption isotherms (Figure 4.1a). The BET surface area evaluated by the adsorption of N_2 was increased from 0.4 to 43.0 $m^2\ g^{-1}$. The pore volume evaluated using the Barret, Joyner and Halenda (BJH) method was increased from 6 x 10^{-4} to 2 x 10^{-3} $cm^3\ g^{-1}$ from untreated to treated carbon (Table 4.1)[8].

These experiments reveal that treated carbon paper presents a great variety of pore sizes. In fact, the high-pressure increase of N_2 adsorption reflects the presence of both mesopores (between 2 and 50 nm diameter) and macropores (above 50 nm) [88, 89]. Furthermore, the pore distribution analysis (Figure 4.1b) also reveals the great number of micropores (below 2 nm diameter). According to this distribution analysis, most pore diameters are between 1 and 4 nm. Therefore, hydrated SO_4^{2-} (7.33 Å) and Na^+ (3.59 Å) ions can easily access the majority of the treated carbon pores [90]. The different scales of porosities (micro, meso and macropores) allows a better accessibility of ions to the surface of the carbon. Macropores serve as ion reservoirs, decreasing

diffusion times to smaller pores. Mesopores serve as pathways to access smaller pores and allow a better rate capability. Micropores present the largest contribution to the surface of the carbon (Table 4.1) [8].

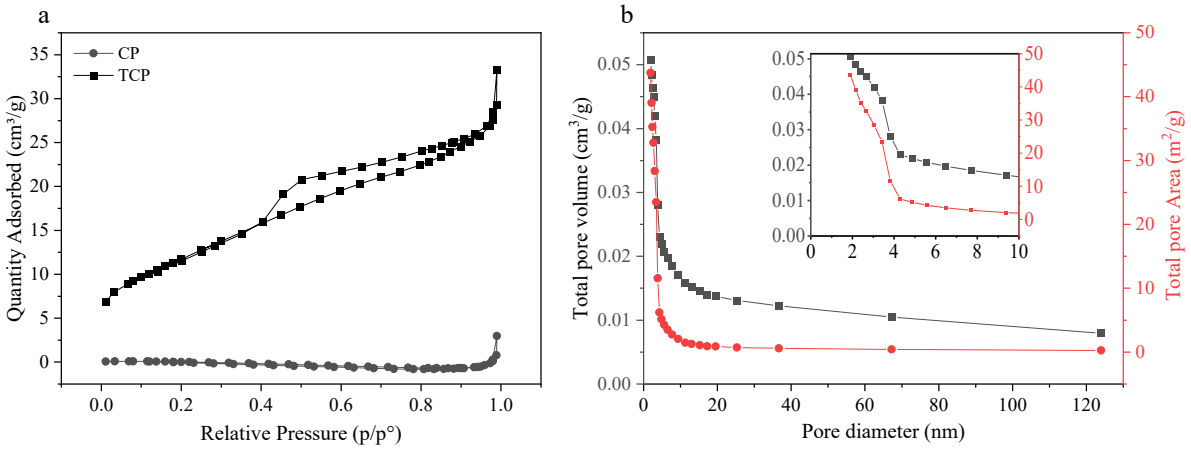

Figure 4.1 a) Adsorption and desorption N_2 isotherms for treated and untreated carbon paper (TCP and CP). b) pore distribution for treated carbon paper: total pore volume and total pore area as a function of pore diameter. Inset: micropore and mesopore enlargement [8].

Table 4.1 Summary of the structural properties of treated and untreated carbon paper (TCP and CP). S_{BET}: BET surface area; S_{Micro}: micropore surface area; V_{micro}: micropore volume; V_{total}: total pore volume; D: average pore diameter [8].

Sample	**S_{BET} (m^2/g)**	**S_{micro} (m^2/g)**	**S_{micro}/S_{BET}**	**V_{total} (cm^3/g)**	**V_{micro} (cm^3/g)**	**V_{micro}/V_{total}**	**D (nm)**
CP	0.37	0.12	0.32	5×10^{-3}	6×10^{-4}	0.12	159
TCP	43.04	38.05	0.88	5×10^{-2}	2×10^{-3}	0.04	5.1

4.1.2 Surface heteroatom functionalization and doping

Sulfuric acid is also responsible for S surface doping (Table 4.2 and Figure 4.2f). The use of nitric acid in the first acid treatment and phosphoric acid in the second introduces N and P surface doping as well as O functionalization (Table 4.2 and Figure 4.2c-e). These alterations of the surface chemistry have two main effects. First, they introduce polarity at the surface of the carbon making treated carbon more wettable to the aqueous electrolytes used in the electrochemical characterization. Second, they introduce redox active functionalities adding pseudocapacitance to the purely electrostatic EDL capacitance of carbon.

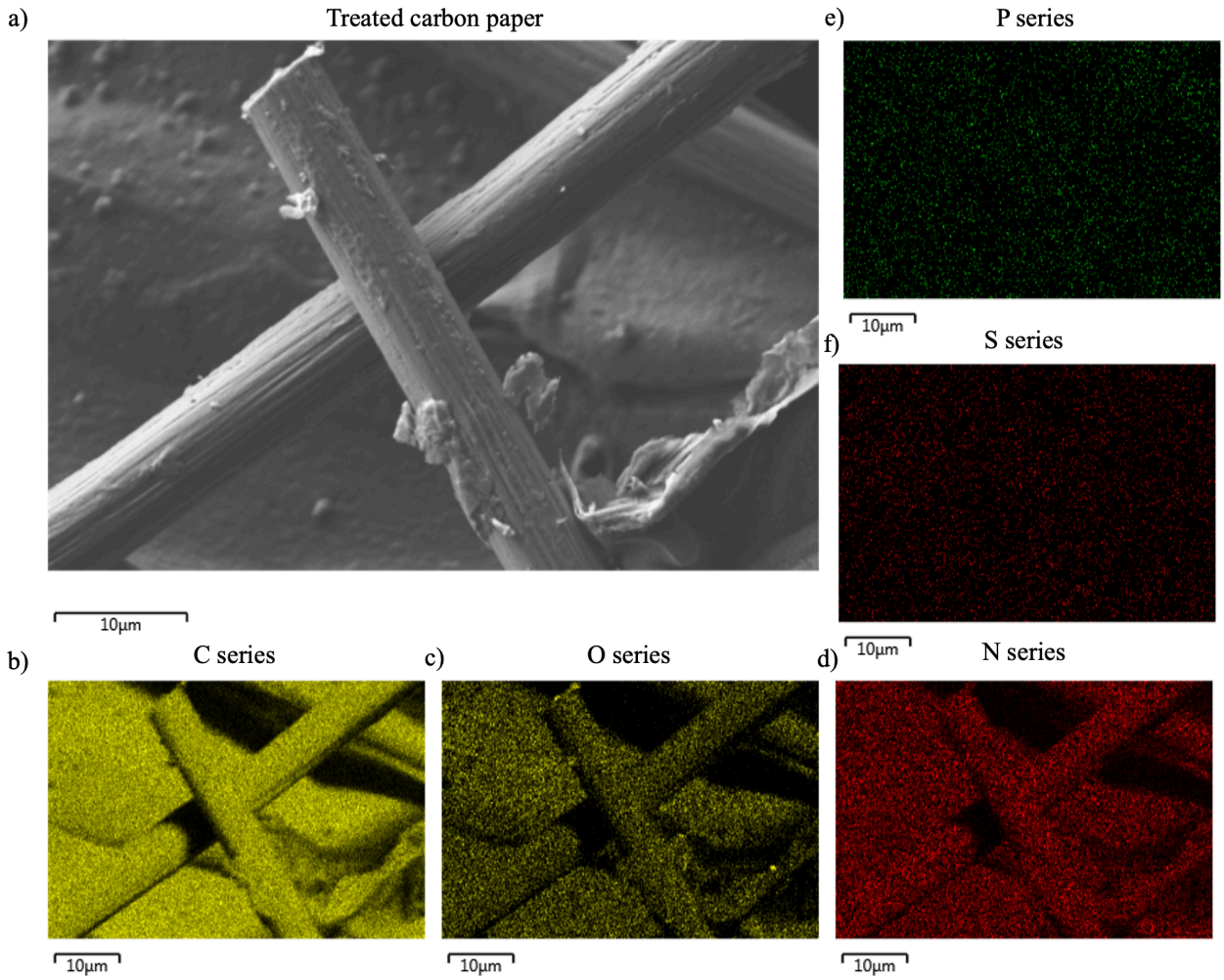

Figure 4.2 EDX investigation of the surface chemistry of treated carbon paper. a) SEM image of the studied area. EDX-revealed atomic presence for b) carbon, c) oxygen, d) nitrogen, e) phosphorus, and f) sulfur. For the SEM, the acceleration voltage is 5 keV.

To observe this O, N, S, and P surface doping, an EDX investigation is conducted on the treated carbon fiber shown in the SEM image in figure 4.1a. EDX images reveal high concentration of O and N (Figure 4.2c and d) as the shape of the investigated carbon fiber can be seen through these atoms just as for the C series (Figure 4.2b). On the other hand, P and S series (Figure 4.2e and f) reveal much smaller concentrations. An XPS investigation was required to quantify the concentration of these heteroatoms.

4.1.2.1 X-ray photo spectroscopy (XPS) investigation

The atomic percentage of C and each doping atom is presented in table 4.2 and the XPS spectra are shown in figure 4.3. As expected from the EDX results: O and N present concentrated surface functionalization and doping (respectively 10 and 8 at. %) whereas S and P are less concentrated (about 1 at. %).

Table 4.2 Atomic percentages of the surface of untreated and treated carbon paper, resulting of an XPS investigation at 1.0 eV energy steps.

ELEMENT		C	O	N	S	P
ATOMIC %	Untreated carbon paper	95	5	0	0	0
	Treated carbon paper	80	10	8	1	1

The XPS survey spectra of untreated carbon paper presents only two remarkable peaks at about 285 and 533 eV, corresponding to C 1s and O 1s respectively (Figure 4.3 and Table 4.3) [8]. On the other hand, the survey scan of treated carbon paper presents three additional peaks

corresponding to P 2p (at 132 eV), S 2p (168 eV), and N 1s (400 eV) confirming the presence of heteroatom doping at its surface. Furthermore, the intensity of the O 1s peak is much larger for treated than untreated carbon paper, confirming further O functionalization through acid oxidation and breaking of C=C bonds. In fact, the deconvolution of the C 1s peak reveals that the concentration of C=C double bonds (binding energy of 284.3 eV) is lower for treated than untreated carbon paper. Conversely the concentration of C-C single bonds (284.8 eV), C-O (286.1 eV), C=O (287.8 eV), and O-C=O (289.0 eV) increases from untreated to treated carbon paper testifying of oxidative breakage of the C=C bonds (Table 4.3) [91, 92].

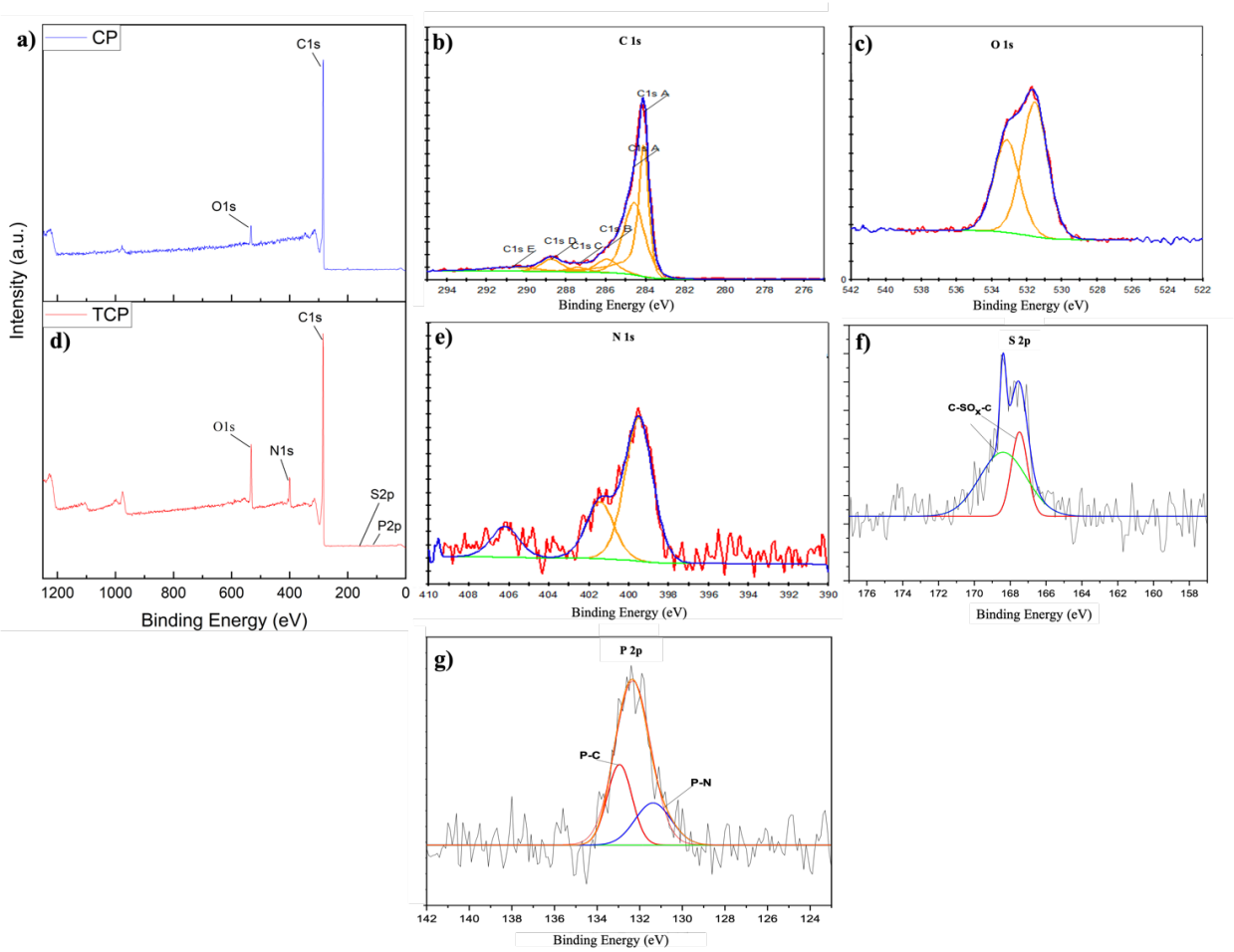

Figure 4.3 XPS survey spectra of a) untreated carbon paper and d) treated carbon paper. Deconvoluted spectra of the b) C 1s signal, c) O 1s signal, e) N 1p signal, f) S 2p signal and g) P 2p signal for the treated carbon paper sample [8].

The O 1s spectrum also shows traces of oxidation resulting from the treatment of the carbon. The peak can be decomposed in three signals: -OH bonds (at 531.8 eV), COOH (533.3 eV), and adsorbed water (534.6 eV). The atomic concentration of the acid function more than triples following the treatment, proof of the oxidative O functionalization.

The N 1s deconvolution spectrum shows three main types of bonds: N–(C-O)–N (at 399.9 eV), N-C (401.9 eV) and planar NO_2 (406.4 eV). These peaks show that N is integrated to the surface of treated carbon paper as both functional groups as well as into the C lattice.

Similarly, the P 2p peak can be separated into P-C (at 131.6 eV) and P-N (133.3 eV) showing that the P is also introduced as functions and in the carbon lattice.

Finally, the S 2p spectrum is mostly due to sulfone groups C–SO_x–C (at 168.2 eV) indicating that the addition of S to the surface is done through O-based S functions at the surface of the carbon.

Table 4.3 High resolution XPS scans of treated and untreated carbon paper (TCP and CP) and identification of the corresponding chemical bonds [8].

Group Name	**Binding energy (eV)**	**Identification**	**Atomic %**	
			CP	TCP
P - 2p	131.60	P-C	--	0.45
	133.30	P-N	--	0.20
S - 2p	168.22	C-SO_x-C	--	1
C - 1s	285.10	element total	94.6	79.79
	284.30	C=C	78.6	31.8
	284.80	C-C	10.2	29.5

	286.10	C-O	0.7	5.5
	287.80	C=O	1.2	1.9
	289.00	O-C=O	0.8	5.1
	291.00	π→π* C=C	3.7	3.9
N - 1s	400.70	element total	--	8.31
	399.90	N-(C-O)-N	--	3.2
	401.90	N-C	--	1.2
	406.40	planar NO_2	--	0.5
O - 1s	533.10	element total	5.1	10.25
	531.80	-OH	--	
	533.30	COOH	1.8	7.7
	534.60	water peak	0.3	--

4.1.3 Effect of the carbon treatment on the capacitance of bare electrodes

These three improvements to carbon paper: increase in specific surface area, improved wettability and doping with electroactive atoms, result in a great (over 1 order of magnitude) increase in capacitance for the bare carbon electrodes (Figure 4.4): from 40 to 620 mF cm^{-2}.

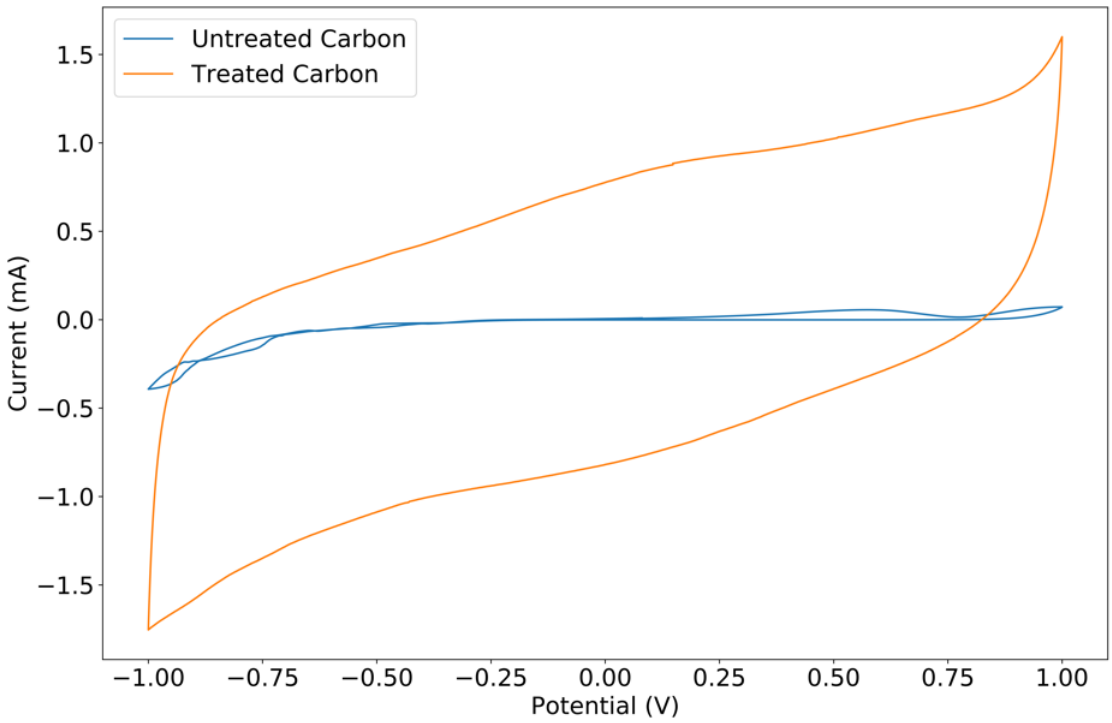

Figure 4.4 Cyclic voltammetry of untreated and treated carbon. The scan rate is 5 mV s^{-1}.

4.2 Comparison of the molecular structures and expected reactivity

The 5 tannins considered in this study can be grouped into three sub-categories based on their molecular structure [25]. Catechin, epicatechin and epicatechin gallate are flavanol derivatives and known as condensed tannins, found in nature as oligomer assemblies. Tannic acid is a hydrolysable tannin and found unmodified in nature. Pyrogallol is a very small phenolic molecule, composed only of the active site of the other molecules. Pyrogallol is produced naturally by some underwater plants [24].

The 5 tannins presented in figure 2.4 present obvious differences (in structure, molecular weight, and number of phenol functions) but several similarities (in structure, functional and active groups, and redox properties) essential to their application in electrochemical energy storage.

The three condensed tannins are flavanol (Figure 4.5a) derived structures, whereas tannic acid is formed by gallic acid molecules linked together by ester bonds and centered around a D-glucose cycle (Figure 4.5b and c). Pyrogallol only presents a vicinal tri-phenol cycle, very similar to a

single catechol (Figure 4.5d). Molecular weights vary from 126 Da for pyrogallol, 290 Da for catechin and epicatechin, 458 Da for epicatechin gallate, to 1 700 Da for tannic acid and are expected to influence the reactivity of their respective tannins. The very small molecular weight of pyrogallol is expected to lead to very fast redox reaction compared to the heavier, branched and less accessible tannic acid. Likewise, phenol densities (theoretical number of phenol functions per gram of tannins) anticipate a decreasing reactivity order of pyrogallol, epicatechin gallate, tannic acid and catechin/epicatechin (23.8, 15.3, 14.7 and 13.7 mmol g^{-1} respectively). However, not all phenol functions can be easily oxidized into a quinone. Considering, the molecular structure of our tannins, only the catechol cycles are expected to react. This supposed reactivity is confirmed for catechin by Janeiro *et al.* [33]. Hence, the supposed reducing potential order becomes: pyrogallol, tannic acid, epicatechin gallate and catechin/epicatechin with 7.9, 5.9, 4.4 and 3.4 mmol g^{-1} of catechol cycles (counting one catechol function for the tris-vicinal phenol of gallic acid derivatives). Thus, when considering the difference in structure (complexity and number/accessibility of branches), molecular weight and reactive site concentration, pyrogallol is expected to achieve the highest performances for electrochemical storage owing to its simple structure, small size, and high catechol concentration. Tannic acid's reactivity is more complex to predict as its highly branched structure and high molecular weight may decrease the accessible number of catechol functions. Finally, catechin, epicatechin and epicatechin gallate, can be seen as more balanced options, combining a relatively small and simple structure with a slightly lower reactive site concentration leading to more stable molecules than pyrogallol. In fact, pyrogallol is known for oxidizing in contact with light and/or air leading to complex reactions and creating bigger molecules, with only part of these oxidation products maintaining their redox activity [93, 94].

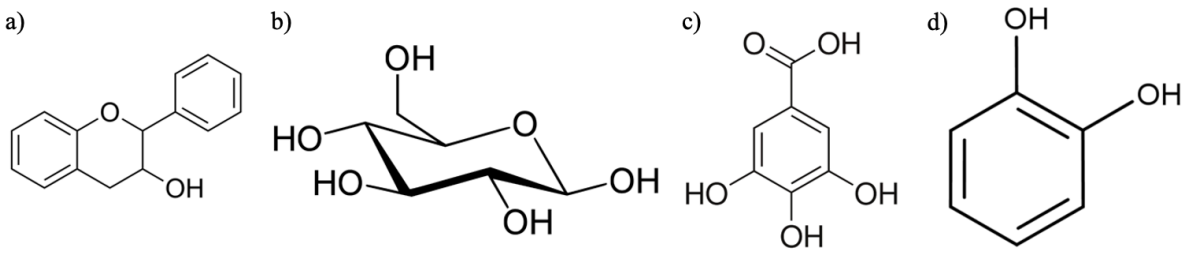

Figure 4.5 Main structural components of the tannins considered in this study. a) flavan-3-ol, b) D-glucose, c) gallic acid and d) catechol.

After considering the molecular differences that make these 5 tannins a good sample of the vast family, let us study the similarities that announce comparable properties for electrochemical energy storage. The three condensed tannins are composed of the same flavan-3-ol core, modified to present a resorcinol and a catechol cycle. Catechin and epicatechin are enantiomers and epicatechin gallate only presents an addition of a gallic acid through an ester bond. This ester-bonded gallic acid addition found again in the branches of tannic acid. Finally, all molecules present catechol functions that can be reversibly oxidized into quinones (Figure 2.5) and none of them present conjugated structures causing poor electronic conductivity.

Following this theoretical investigation, we can expect similar electrochemical reactivity from our diverse pool of tannins, when depositing them on carbon electrodes to test their application to electrochemical capacitors. We expect small variations in surface morphology, capacitance performance, notable potentials, and device stability.

4.3 Surface morphology

We drop-casted concentrated tannin solution on treated carbon paper and proceeded to characterize their surface morphology using SEM. The first SEM images show that tannins do not form any noticeable structures on carbon (as shown for the case of catechin on Figure 4.6). Furthermore, their constituting atoms are not differentiable from those of the carbon paper (e.g. through EDX or XPS). Therefore, we reveal their presence by staining, exploiting the reducing properties of tannins (polyphenols) on heavy metal cations, such as silver (Figure 4.7) [79, 95, 96].

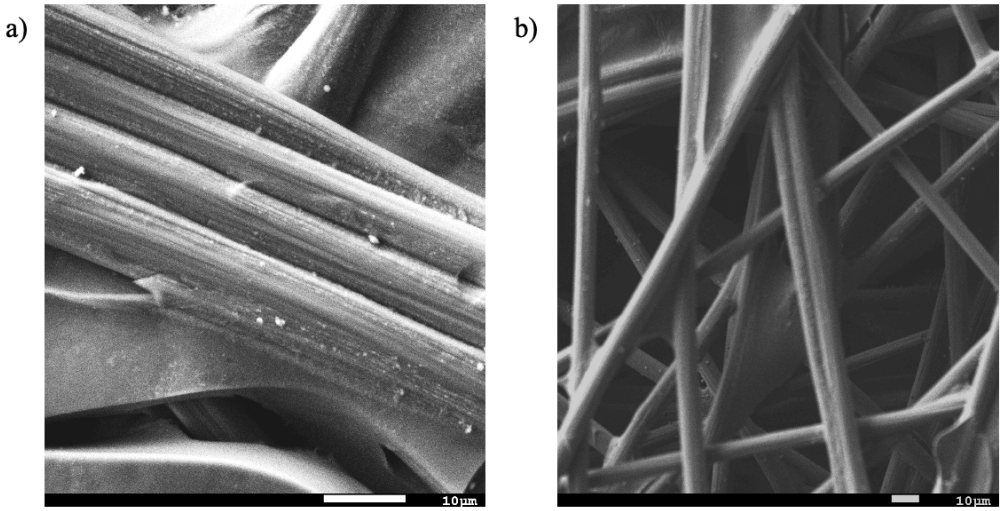

Figure 4.6 SEM images of a) treated carbon paper and b) catechin on treated carbon paper. Acceleration voltage is 5 kV in backscattered electron mode.

The stained treated carbon sample does not present any metallic silver deposits (Figure 4.7a) proving that it is the reducing phenol molecules (tannins) that are reacting with the silver cations. Indeed, the stained tannin samples present a dense covering of silver nanoparticles associated with the presence of chemically reducing polyphenol molecules. Catechin, epicatechin and pyrogallol (Figures 4.7b, c and d) reveal a denser tannin cover than tannic acid and epicatechin gallate (Figures 4.7e and f). This difference can be attributed to several factors. The molar loading is higher for small molecules since the mass loading was equal for all five tannins; for instance, the molar

loading was about 10 times higher for pyrogallol than tannic acid. Further, small molecules can more efficiently be accessed by silver cations.

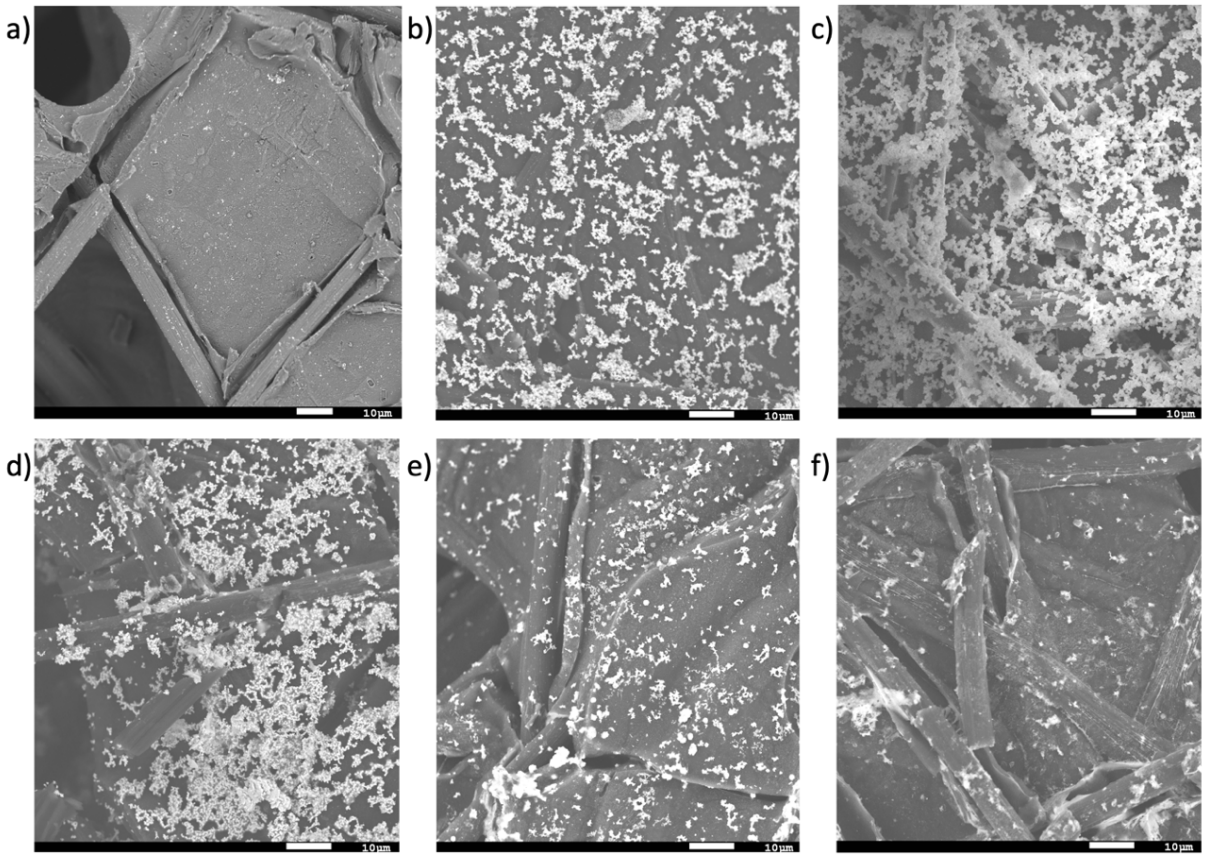

Figure 4.7 SEM images of silver-nitrate-stained samples of treated carbon and tannins on treated carbon. Images of a) stained treated carbon, without tannins, b) catechin, c) epicatechin, d) pyrogallol, e) tannic acid and f) epicatechin gallate. Acceleration voltage is 5 kV in backscattered electron mode.

To confirm that the white particles observed on the stained tannin-on-carbon samples were in fact silver and not edge effects, we compared the EDX scan of two different regions (Figure 4.8).

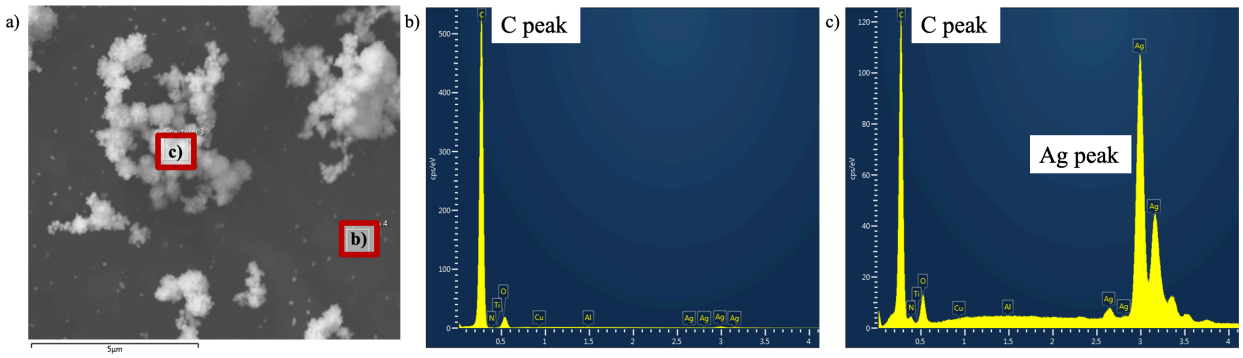

Figure 4.8 Compared EDX scan of two regions of the stained catechin-on-carbon sample. a) SEM image at 5 keV of the stained catechin on carbon. b) Region without visible particles, c) region supposed to present dense silver concentration.

Finally, SEM images show that the addition of tannic acid as a binder [38] does not significantly alter the surface of the catechin/tannic acid sample (Figure 4.8).

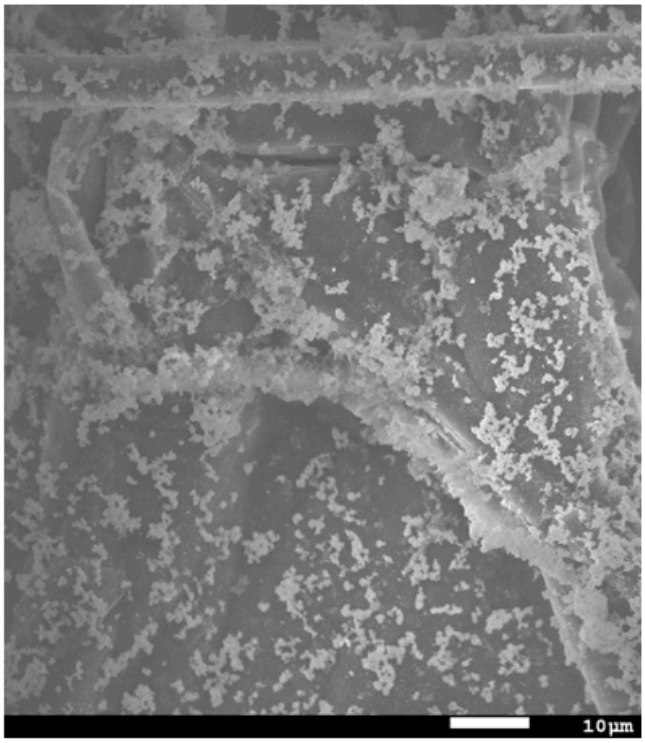

Figure 4.9 SEM image of silver-nitrate-stained samples of catechin/tannic acid on treated carbon. Acceleration voltage is 5 kV in backscattered electron mode.

4.4 Electrochemical characterization

A cyclic voltammetry investigation is conducted for single electrodes in a three-electrode setup. Na_2SO_4 (0.5 M) is used as electrolyte, allowing to work at near neutral pH (about 6) to achieve more environmentally friendly devices compared to the lithiated or acidic electrolytes commonly used in organic electrochemical capacitors.

4.4.1 Deposition of tannins on untreated carbon

When deposited on untreated carbon, the studied tannins bring about contrasted capacity enhancements. In the cyclic voltammetry presented in figure 4.10a the mass loading is 0.3 mg per electrode (0.6 mg cm^{-2}). When increasing the mass loading, the capacity enhancement drops for all tannins and even becomes negative. Already, at this lower mass loading two tannins: catechin and pyrogallol result in a decrease in capacity (Figure 4.10b).

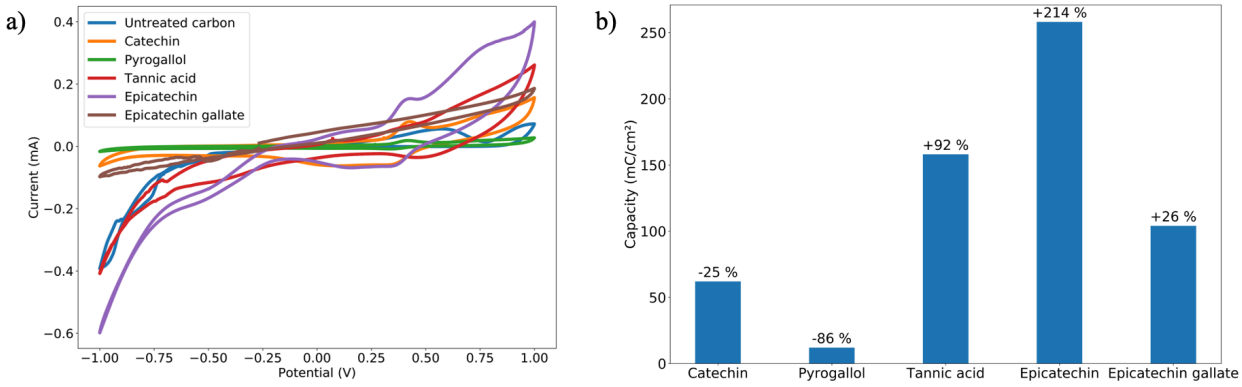

Figure 4.10 a) Cyclic voltammetry for tannins deposited on untreated carbon (the 3rd cycle is reported because the first two cycles present significant differences with respect to the rest due to partial desorption of the deposited tannin), sweeping rate 5 mV s^{-1}, 0.5 M $Na_2SO_{4(aq)}$ b) Comparative capacitance for tannin-loaded untreated carbon electrodes. Percentages represent the capacitance increase compared to the corresponding bare untreated carbon electrodes. The mass loading is 0.6 mg cm^{-2}.

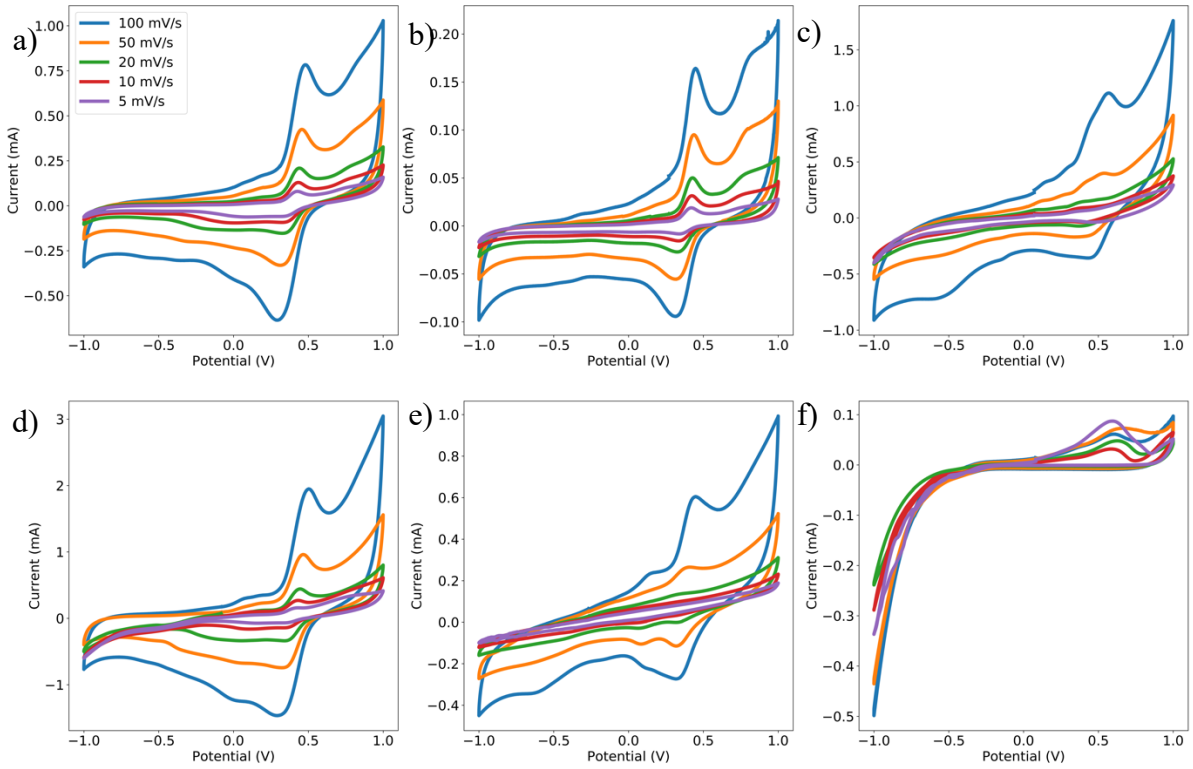

Figure 4.11 Cyclic voltammograms of tannins on untreated carbon at 100, 50, 20, 10 and 5 mV s^{-1} scan rates. a) catechin, b) pyrogallol, c) tannic acid, d) epicatechin, e) epicatechin gallate, f) Untreated carbon. Electrolyte is $Na_2SO_{4(aq)}$.

These decrease in capacity following the deposition of catechin or pyrogallol on untreated electrodes is attributed to the formation of an insulating layer of tannins. In fact, tannins are non-conjugated molecules and, to date, no evidence of π-π stacking is found in literature to help inter-molecular electronic conductivity. The increase in capacity upon depositing tannic acid or epicatechin gallate is attributed to the smaller molecular loading (no insulating layer) of these bigger molecules. SEM confirms a denser coverage of the carbon by small molecules (catechin, epicatechin, pyrogallol) than larger ones (epicatechin gallate, tannic acid). The large increase in capacity granted by epicatechin contrasts with the poor performance of its enantiomer. This is attributed to the lesser adsorption affinity of epicatechin than catechin resulting in rapid desorption when the electrode is dipped in the cell electrolyte thus, a lower effective mass loading [36].

A second shortcoming of the tannin-on-untreated carbon electrodes is their lack of stability over the entire studied potential window. The entire -1 to 1V range was studied to compare these results to the ones obtained using treated carbon but clear instabilities are visible towards the extremities of the potential window. The region below – 0.25 V (vs Ag/AgCl) shows a current drop due to instability of the carbon paper. The electrodes coated with the tannins with the bigger molar loading (pyrogallol and catechin) create an insulating layer preventing access to the carbon paper and thus promoting its stability at lower potentials.

Nonetheless, a full cyclic voltammetry investigation of tannin-on-untreated carbon electrodes was conducted and is presented in figure 4.11. The cyclic voltammetry presents very distinctive peaks characteristic of battery-like materials at about 0.4 to 0.5 V for oxidation and 0.3 to 0.4 V for reduction (Table 4.4). These peaks are attributed to the catechol-catequinone reversible oxidation present in all 5 tannins.

Table 4.4 Oxidation and reduction potentials (vs. Ag/AgCl) for the 5 considered tannins on untreated carbon. Peak potentials are measured at a 5 mV s^{-1} scan rate in $Na_2SO_{4(aq)}$ electrolyte.

Location of the redox signal	Catechin	Pyrogallol	Tannic acid	Epicatechin	Epicatechin gallate
Oxidation	0.4 V	0.4 V	0.5 V	0.4 V	0.2 and 0.4 V
Reduction	0.3 V	0.3 V	0.4 V	0.3 V	0.1 and 0.3 V

4.4.2 Deposition of tannins on treated carbon

Following these preliminary results on untreated carbon paper, the same study was conducted for tannin-on-treated carbon paper electrodes.

Owing to the larger specific surface area of the treated carbon (43.0 instead of 0.4 m^2 g^{-1}), the mass loading could be increased to 1.5 mg per electrode (3 mg cm^{-2}) while maintaining increasing

capacity enhancement. Furthermore, the treated carbon electrodes are stable over the entire -1 to 1V potential window. This improved stability is attributed to the better wettability allowing for better electrolyte ion accessibility (Figure 4.12a).

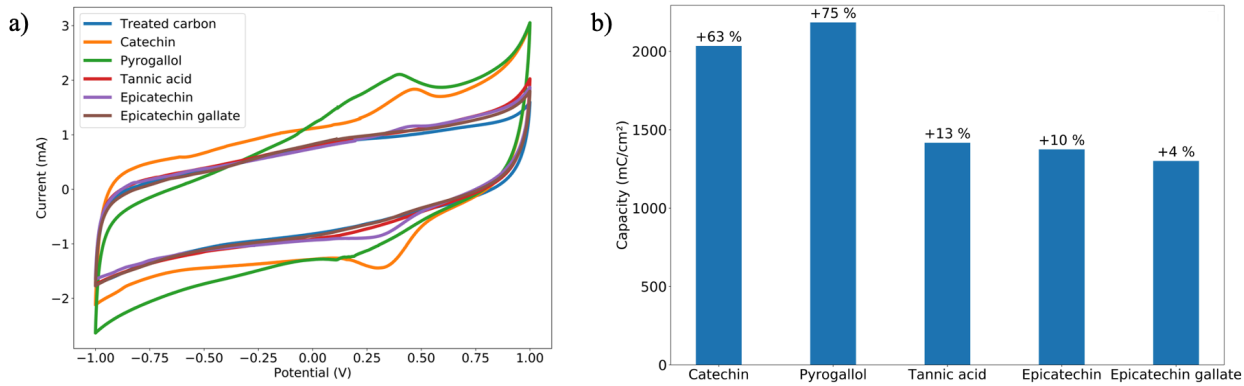

Figure 4.12 a) Cyclic voltammetry for tannins deposited on treated carbon (the 3rd cycle is reported because the first two cycles present significant differences with respect to the rest due to partial desorption of the deposited tannin), sweeping rate 5 mV s^{-1}, 0.5 M $Na_2SO_{4(aq)}$ b) Comparative capacitance for tannin-loaded treated carbon electrodes. Percentages represent the capacitance increase compared to the corresponding bare treated carbon electrodes. The mass loading is 3 mg cm^{-2}.

The capacity enhancement trend is inverted compared to the results found on untreated carbon (Figure 4.12b). The smaller molecules, catechin and pyrogallol, present the highest capacity improvements, while the larger, tannic acid and epicatechin gallate, the lowest. Again, the two enantiomers, catechin and epicatechin behave in opposite ways. The very high specific surface area is thought to prevent the formation of an insulating layer by presenting larger quantities of adsorption sites directly on the surface of the carbon. The lower improvement brought about by the larger tannins is attributed to the uneven coverage of the carbon fibers. Finally, epicatechin's lower capacity improvement is attributed to its lower adsorption affinity on carbon resulting in a lower effective mass loading.

Figure 4.13 presents cyclic voltammetry at different scan rates for all tannins on treated carbon. This cyclic voltammetry investigation reveals that the peaks found when tannins were deposited on carbon are changed to broader features and quasi-rectangular shapes like pseudocapacitive

materials. To verify the possible pseudocapacitive behavior of the tannin-on-treated carbon electrodes, an extensive cyclic voltammetry study was conducted to identify the limiting charge storage mechanism.

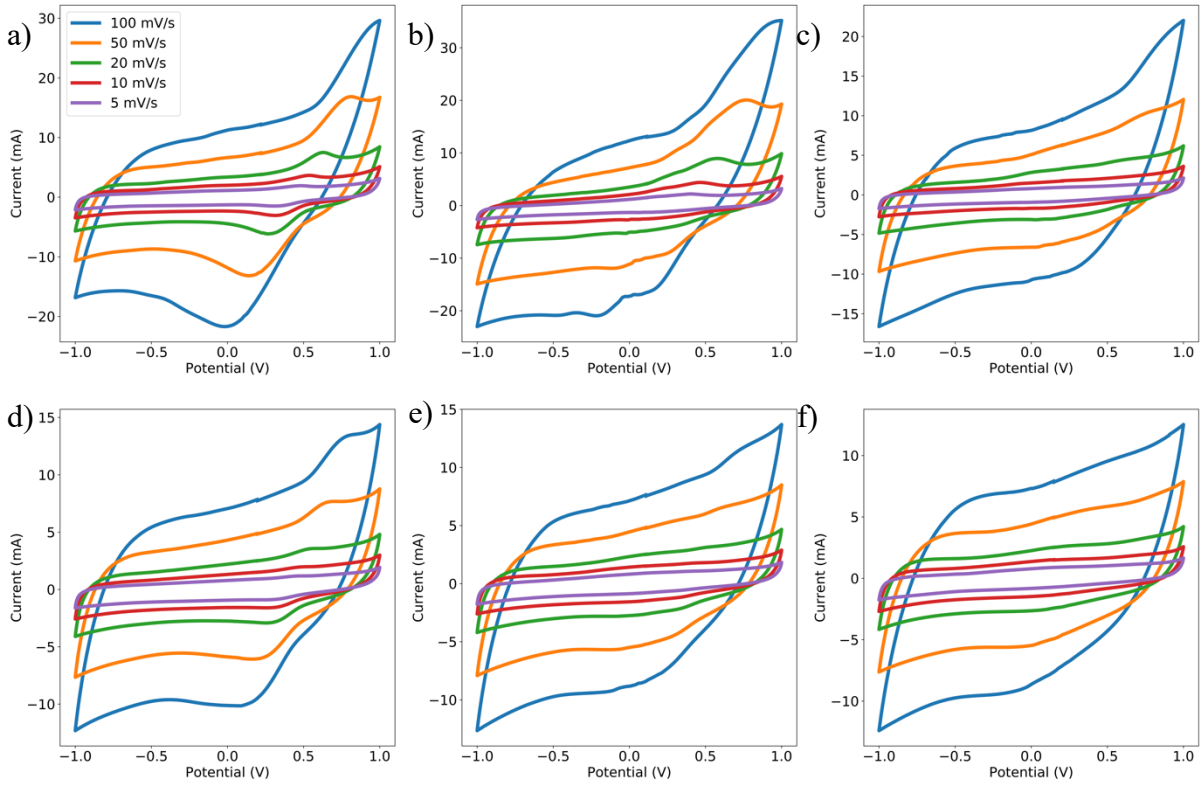

Figure 4.13 Cyclic voltammograms of tannins on treated carbon at 100, 50, 20, 10 and 5 mV s^{-1} scan rates. a) catechin, b) pyrogallol, c) tannic acid, d) epicatechin, e) epicatechin gallate, f) Treated carbon. Electrolyte is $Na_2SO_{4(aq)}$.

4.4.3 Limiting charge storage mechanisms for tannin-on-carbon electrodes

To determine the limiting charge storage mechanisms of our tannin-on-untreated carbon and tannin-on-treated carbon electrodes, we used the logarithmic form of equation 2.2 to link the peak current to the scan rate:

$$\log i \approx \log a + b \log v$$

where i the peak current intensity, v the scan rate, and a and b constants. As specified in chapter 2, b is close to 1 for pseudocapacitive materials (voltametric current limited by electron transfer rate) and 0.5 for battery-like materials (voltametric current limited by diffusion rate) [18].

Catechin-based electrodes were used for this study for several reasons. First, catechin retains distinguishable redox features when deposited on treated carbon. Second, pyrogallol-based electrodes (who also retains these features) are less stable than catechin ones due to the light and air assisted oxidation of pyrogallol. Scan rates of 1, 2, 5, 7, 10, 20, 30, 40, and 50 mV s^{-1} were studied to have over one order of magnitude range. Catechin on treated carbon presents a peak at about 0.6 V vs. Ag/AgCl (Figure 4.14a). For catechin on untreated carbon, low scan-rate voltammograms also show a peak at about 0.4 V, that becomes a shoulder at higher scan rates (20 mV s^{-1} and above) (Figure 4.14b). For these scan rates, we measured the current at the inflection point of the shoulder, to be coherent with the potential measurements of lower scan rates (Table 4.5).

Table 4.5 Oxidation peak currents for catechin on untreated and treated carbon for different scan rates. Experiments are carried out in $Na_2SO_{4(aq)}$ electrolyte.

Scan Rate (mV s^{-1})	1	2	5	7	10	20	30	40	50
Untreated carbon current (mA)	0.025	0.035	0.055	0.065	0.085	0.150	0.170	0.200	0.250
Treated carbon current (mA)	0.40	1.00	1.80	2.10	3.00	5.50	8.50	12.00	16.00

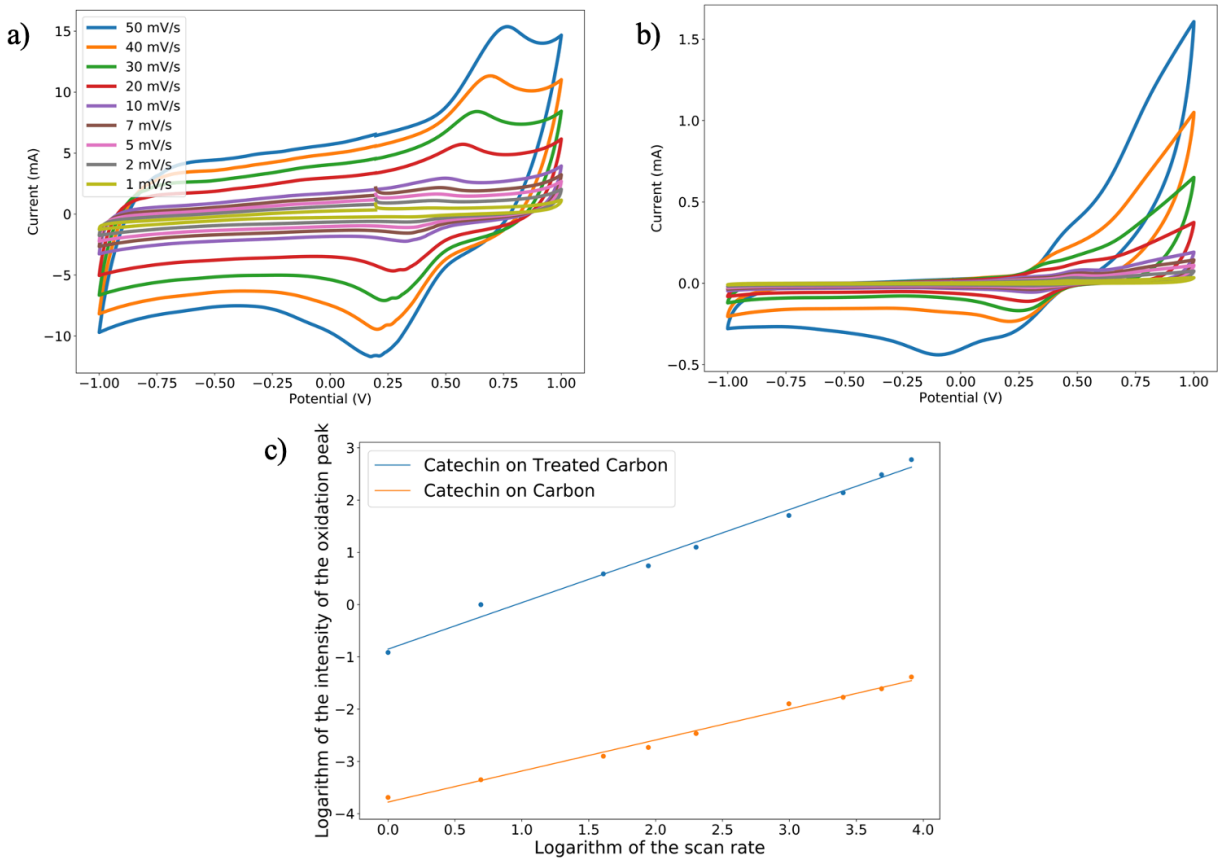

Figure 4.14 Cyclic voltammetry at 50, 40, 30, 20, 10, 7, 5, 2 and 1 mV s^{-1} for catechin on a) treated and b) untreated carbon. c) Evolution of the logarithm of the oxidation peak intensity as a function of the logarithm of the scan rate. The b-value (slope) is 0.9 for treated carbon and 0.6 for untreated. R^2 values are 0.989 and 991 for treated and untreated carbon, respectively.

We found b-values of 0.6 and 0.9 for catechin on untreated and treated carbon, respectively (Figure 4.14c). The b-value close to 0.5 in the former case indicates the kinetics of catechin on untreated carbon are controlled by the ion diffusion whereas on treated carbon the electron transfer rate becomes the limiting process [97, 98]. The b-value close to 0.5 for catechin-on-untreated carbon paper leads to classify tannins as battery-like materials whose charge storing performance should therefore be reported in C or mAh. However, the larger specific surface area of the treated carbon paper leads to thinner layers of tannins (fivefold loading increase for a hundredfold surface increase – see experimental chapter) and a better accessibility for electrolyte ions, allowing the resulting

electrodes to exhibit pseudocapacitive-like behavior. In other words, tannins-on-treated carbon paper behave as extrinsic pseudocapacitive materials: they feature pseudocapacitive-like behavior due to the fabrication process but not their intrinsic property [20]. We make use of this extrinsic capacitance to use capacitance (in F g^{-1} or mF cm^{-2}) to report the performance of the electrochemical capacitor device presented in chapter 5 as it is more commonly used in literature for such devices. This allows us to compare the performance of tannins with other existing electrochemical capacitors based on organic materials.

CHAPTER 5 TANNIN-ON-CARBON ELECTROCHEMICAL CAPACITORS

5.1 Tannin-on-carbon electrochemical capacitors

The pseudocapacitive-like behavior of the tannin-on-carbon electrodes resulting from the treatment of the carbon paper makes them suitable for electrochemical capacitor applications, which we proceeded to explore.

5.1.1 Catechin-based electrochemical capacitors

We focused on catechin, the second most promising candidate (after pyrogallol) from single-electrode studies in terms of capacity/capacitance enhancement. Pyrogallol electrodes presented the highest relative capacity/capacitance increase when deposited on treated carbon, however, this improvement rapidly fades (few hundred cycles). This is attributed to the auto-oxidation of pyrogallol creating macromolecules that are neither conjugated (electronically conductive) nor feature the redox active catechol functional group [93, 94]. Catechin combines significant capacity/capacitance enhancement and relative cycling stability.

5.1.2 Cycling stability challenges

Despite the better stability of catechin as a molecule (no parasitic reactions), the cycling stability of catechin-based devices is very poor. Upon cycling for more than a few hundred cycles, an orange color appears in the electrolyte due to catechin desorption. Therefore, we included tannic acid for its hidrogen-bonding binding properties [38] in the formulation of the electrode material to promote the cycling stability of the catechin devices. This tannin blend proved effective, resulting in perfect cycling stability for over 5 000 cycles.

5.2 Symmetric aqueous electrochemical capacitor performance

5.2.1 Capacitance and comparison to the state of the art

The cyclic voltammetry in electrochemical capacitor configuration display quasi-rectangular shapes, in accordance with the extrinsic pseudocapacitance expected from the catechin-on-treated carbon paper electrodes (Figure 5.1a). Likewise, the galvanostatic charge and discharge presents a quasi-triangular shape (Figure 5.1b). The catechin/tannic acid device presents broad redox features at about 0.5 and 0.2 V vs. Ag/AgCl for oxidation and reduction, respectively.

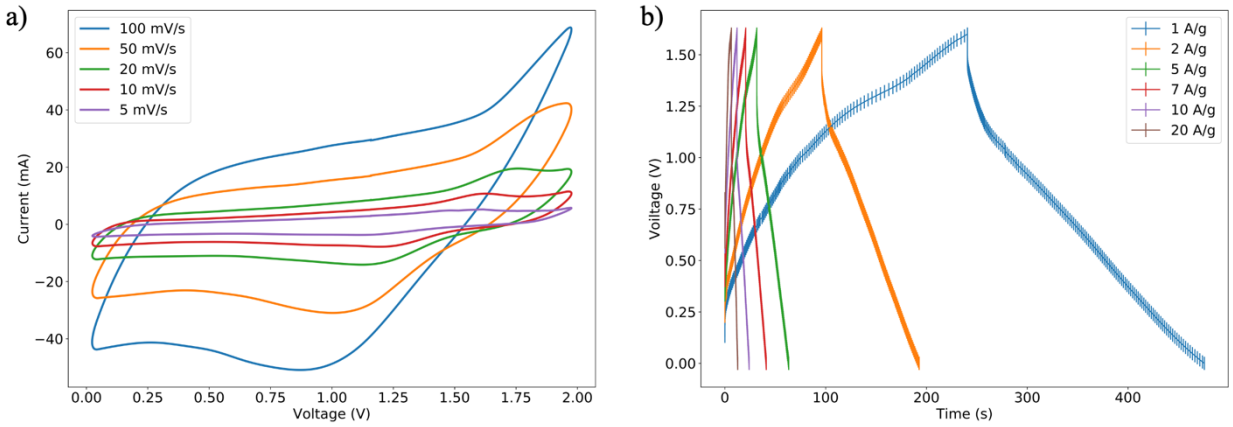

Figure 5.1 Electrochemical characterization of the catechin/tannic acid aqueous symmetric electrochemical capacitor. a) cyclic voltammetry at 100, 50, 20, 10, and 5 mV s^{-1} scan rates, b) galvanostatic charge and discharge at 1, 2, 5, 7, 10, and 20 A g^{-1}.

A comparative study, with a reference electrochemical capacitor made from bare treated carbon electrodes is conducted (Figure 5.2). From the voltametric study (Figure 5.2a), we measured an improvement for the capacitance from 478 mF cm^{-2} for bare treated carbon, to 648 mF cm^{-2} (+36 %) for catechin/tannic acid (calculated from cyclic voltammetry at a 5 mV s^{-1} scan rate). When normalized to the mass of deposited tannins, this capacitance corresponds to 216 F g^{-1} which is a notable values for biosourced organic materials [99]. Capacitances of 360 F g^{-1} were reported for carbonized benzoquinone-amines [100], 170 F g^{-1} for lignin on activated carbon [101], and 270 F

g^{-1} for polyaniline/tannic acid on reduced graphene oxide [102]. However, these devices make use of acid electrolytes and/or conductive polymers whereas our electrochemical capacitors perform at near-neutral pH.

Galvanostatic charge-discharge curves present quasi-triangular shapes often associated to pseudocapacitive materials (Figure 5.2b). A small ohmic drop of about 20 mV (at 1 A g^{-1}) is present, corresponding to an equivalent series resistance of about 10 ohms. Nyquist plots confirm a capacitive behavior through a nearly vertical diffusion line in the low frequency region. The high frequency region is in accord with a low equivalent series resistance found using galvanostatic curves (Figure 5.2c) [86]. The capacitance retentions is of 50% when increasing the current density from 1 to 20 A g^{-1} (Figure 5.2d).

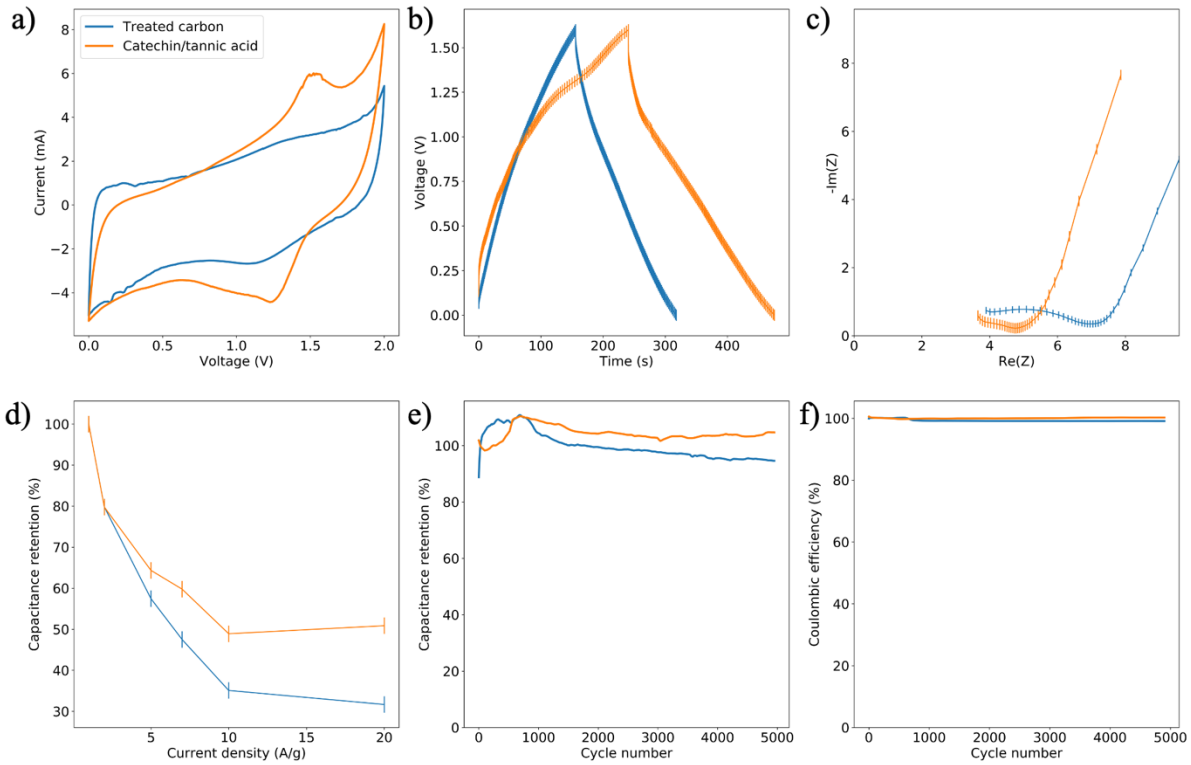

Figure 5.2 Characterization of our catechin/tannic acid aqueous electrochemical capacitor. a) Cyclic voltammetry at 5 mV s^{-1} scan rate, b) galvanostatic charge and discharge at 1 A g^{-1} current density, c) Nyquist plot from 10 Hz to 10 kHz, d) capacitance retention of the device for a current density increase from 1 to 20 A g^{-1}, e) cycling stability of the capacitance as percentage of the average capacitance of the first 50 cycles, f) Coulombic efficiency of the device.

After 5 000 cycles at 20 A g^{-1}, the cycling stability is over 100% for capacitance and 100% for Coulombic efficiency (Figure 5.2e and f). The observed initial capacitance increase is attributed to galvanostatic activation of the carbon during the first cycles [44] as confirmed by the cycling stability curve of the bare treated carbon device (current density was chosen to have the same areal current of 60 mA cm^{-2} as the catechin/tannic acid-based device).

5.2.2 Energy and power densities

We present the specific power and energy density performance of the catechin/tannic acid symmetric electrochemical capacitor in the Ragone plot of figure 5.3. The considered mass is the sum of the deposited tannins and of the tannin-covered carbon paper.

The device achieves good power density, coupled with battery-level energy density. The maximal power and energy densities are 43 kW kg^{-1} and 54 Wh kg^{-1} respectively. These very high energy densities place the catechin/tannic acid device at the limit between electrochemical capacitors and batteries [4]. The maximal power density, although less impressive, remains notable for fully organic electrochemical capacitors [4, 103].

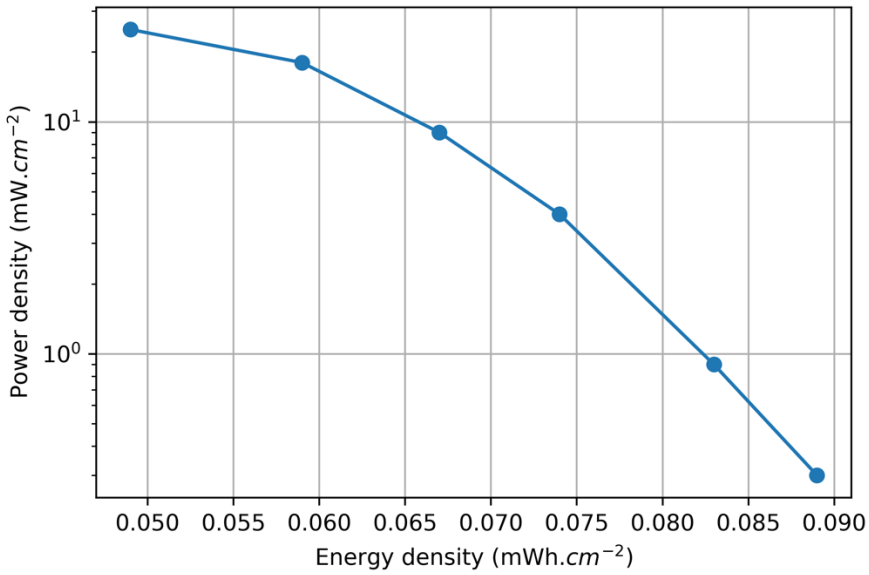

Figure 5.3 Ragone plot for catechin/tannic acid symmetric aqueous electrochemical capacitor (0.5M $Na_2SO_{4(aq)}$ electrolyte).

CHAPTER 6 CONCLUSION, CHALLENGES AND PERSPECTIVES

6.1 Conclusion

The parallel development of intermittent renewable energies and electric vehicles results in a surge in electrochemical energy storage demand. Considering sustainability goals, electrochemical energy storage should include routes based on less polluting, biosourced organic alternatives. However, this requires considerable effort to fill the performance gap between devices based on organic and inorganic materials. Tannins are abundant, low-cost organic materials easily extracted from a great diversity of plant precursors. In this Master of Science work, we selected five members (catechin, pyrogallol, tannic acid, epicatechin, and epicatechin gallate) of the tannin family to devise the molecular features that influence the charge storage performance of devices based thereon. This thesis states that tannins are of interest for sustainable electrochemical energy storage.

Using concentrated aqueous tannin solutions, we drop-casted selected tannins on carbon electrodes to study their redox activity by adopting a simple route to fabricating high-capacity tannins-on-carbon electrodes. The surface area and wettability of carbon paper were increased using a thermal and chemical treatment. A symmetric electrochemical capacitor based on a catechin/tannic acid tannin blend in a near-neutral aqueous electrolyte was fabricated and its charge storage performance evaluated. Finally, by comparing the molecular structures and the performances of the different tannins, the molecular characteristics most suitable to energy storage applications were identified.

Pyrogallol-based electrodes presented the highest capacity, as expected by the high catechol density in the molecule. Conversely, tannic acid and epicatechin gallate, larger molecular weight and more branched candidates, presented lower capacitance. Catechin and epicatechin, although enantiomers, performed very differently, due to their different adsorption properties on carbon paper. Epicatechin brought about little improvement to the capacitance of treated carbon paper while catechin was the optimal candidate for electrochemical storage, leading to a capacitance almost as good as pyrogallol while remaining more stable (no parasitic oxidation).

The catechin/tannic acid device presented promising performance for a fully organic device. It reached a capacitance of 648 mF cm^{-2} (216 F g^{-1}). The Coulombic efficiency and cycling stability

were maintained at 100% for 5 000 cycles. A maximal power density of 43 kW kg^{-1} and maximal energy density of 54 Wh kg^{-1} are reported. These figures of merit place tannins among the best performing organic molecules for electrochemical capacitors.

6.2 Challenges

The use of tannins for sustainable electrochemical energy storage is undoubtably promising. However, like most biosourced molecules, tannins pose major challenges as to their widespread usage.

The low electronic conductivity of tannin-based materials hinders the capacitive enhancement of tannins on certain current collectors such as untreated (low surface area) carbon paper due to the formation of poorly conducting thick deposits.

This work focused on the intrinsic properties of tannins and tried to present a route as environmentally friendly as possible. Thus, conductive additives, that are not environmentally benign, although commonly used in organic/biosourced electrochemical capacitors, where not considered.

Furthermore, the relatively high aqueous solubility of the smaller (most performing) tannins results in desorption from the carbon electrode when used in aqueous electrochemical capacitor configuration. Tannic acid proved an effective binder and allowed considerable cycling stability for electrochemical capacitors making use of organic/biosourced molecules.

6.3 Perspectives and further work

In this work we have shown that tannins represent an opportunity as materials for green electrochemical storage by presenting a catechin-based high performance electrochemical capacitor. However more fundamental work is necessary to achieve state of the art performance using tannin-based devices.

The use of tannic acid's hydrogen-bonding properties to address the cycling stability issues faced by aqueous-state devices proved effective. However, better options may come from studying the adhesion mechanism of tannins on carbon, notably the possibility of engineered π-π stacking. Furthermore, catechin in nature forms oligomer macromolecules whose adhesion properties may be stronger while retaining the reactivity of catechin.

Finally, the tannin-based devices studied present good power densities and very high energy densities for organic electrochemical capacitors. Combining the apparent high energy density of tannins with their good aqueous solubility can be interesting for redox-flow batteries.

REFERENCES

1. P. Poizot, J. Gaubicher, S. Renault, L. Dubois, Y. Liang, and Y. Yao, *Opportunities and Challenges for Organic Electrodes in Electrochemical Energy Storage.* Chemical Reviews, 2020. **120**(14): p. 6490-6557.
2. M.d.P. Pablo-Romero, R. Pozo-Barajas, and R. Yñiguez, *Global changes in residential energy consumption.* Energy Policy, 2017. **101**: p. 342-352.
3. A. Yu, V. Chabot, and J. Zhang, *Electrochemical Supercapacitors for Energy Storage and Delivery* Electrochemical Energy Storage and Conversion, ed. J. Zhang. 2017: CRC Press.
4. P. Simon and Y. Gogotsi, *Materials for electrochemical capacitors*, in *Nanoscience And Technology: A Collection of Reviews from Nature Journals*. 2010, World Scientific. p. 320-329.
5. V. Butsic, M. Baumann, A. Shortland, S. Walker, and T. Kuemmerle, *Conservation and conflict in the Democratic Republic of Congo: The impacts of warfare, mining, and protected areas on deforestation.* Biological Conservation, 2015. **191**: p. 266-273.
6. S. Zhang, Y. Ding, B. Liu, and C.C. Chang, *Supply and demand of some critical metals and present status of their recycling in WEEE.* Waste Manag, 2017. **65**: p. 113-127.
7. T. Brousse, C. Cougnon, and D. Bélanger, *Grafting of Quinones on Carbons as Active Electrode Materials in Electrochemical Capacitors.* Journal of the Brazilian Chemical Society, 2018.
8. A. Gouda, A. Masson, F. Soavi, and C. Santato, *Melanins and tannins solution-deposited on modified carbon paper for high performance 1.6 V aqueous electrochemical capacitors.* Submitted.
9. K. Khanbabaee and T. van Ree, *Tannins: Classification and definition.* Natural Product Reports, 2001. **18**(6): p. 641-649.
10. T. Ghigo, I. Rabin, and P. Buzi, *Black Egyptian inks in Late Antiquity: new insights on their manufacture and use.* Archaeological and Anthropological Sciences, 2020. **12**(3): p. 70.
11. K. Macáková, V. Kolečkář, L. Cahlíková, J. Chlebek, A. Hošťálková, K. Kuča, D. Jun, and L. Opletal, *Chapter 6 - Tannins and their Influence on Health*, in *Recent Advances in Medicinal Chemistry*, R. Atta ur, M.I. Choudhary, and G. Perry, Editors. 2014, Elsevier. p. 159-208.
12. J. Temmink, J.A. Field, J. Van Haastrecht, and R. Merkelbach, *Acute and sub-acute toxicity of bark tannins in carp (Cyprinus carpio L.).* Water Research, 1989. **23**(3): p. 341-344.
13. H. Abruña, Y. Kiya, and J. Henderson, *Batteries and electrochemical capacitors.* Physics Today - PHYS TODAY, 2008. **61**.
14. J.R. Miller and P. Simon, *Electrochemical capacitors for energy management.* Science Magazine, 2008. **321**(5889): p. 651-652.

15. *Allen J. Bard and Larry R. Faulkner, Electrochemical Methods: Fundamentals and Applications, New York: Wiley, 2001, 2nd ed.* Russian Journal of Electrochemistry, 2002. **38**(12): p. 1364-1365.

16. L. Caizán-Juanarena, C. Borsje, T. Sleutels, D. Yntema, C. Santoro, I. Ieropoulos, F. Soavi, and A. ter Heijne, *Combination of bioelectrochemical systems and electrochemical capacitors: Principles, analysis and opportunities.* Biotechnology Advances, 2020. **39**: p. 107456.

17. T. Brousse, D. Bélanger, and J. Long, *To Be or Not To Be Pseudocapacitive?* Journal of the Electrochemical Society, 2015. **162**: p. A5185-A5189.

18. Y. Jiang and J. Liu, *Definitions of Pseudocapacitive Materials: A Brief Review.* ENERGY & ENVIRONMENTAL MATERIALS, 2019. **2**(1): p. 30-37.

19. E. Frackowiak and F. Béguin, *Carbon materials for the electrochemical storage of energy in capacitors.* Carbon, 2001. **39**(6): p. 937-950.

20. V. Augustyn, P. Simon, and B. Dunn, *Pseudocapacitive oxide materials for high-rate electrochemical energy storage.* Energy & Environmental Science, 2014. **7**(5): p. 1597-1614.

21. J. Wang, J. Polleux, J. Lim, and B. Dunn, *Pseudocapacitive Contributions to Electrochemical Energy Storage in TiO2 (Anatase) Nanoparticles.* The Journal of Physical Chemistry C, 2007. **111**(40): p. 14925-14931.

22. D. Hathway, *Oak-bark tannins.* Biochemical Journal, 1958. **70**(1): p. 34-42.

23. A. Mukhopadhyay, Y. Jiao, R. Katahira, P.N. Ciesielski, M. Himmel, and H. Zhu, *Heavy Metal-Free Tannin from Bark for Sustainable Energy Storage.* Nano Letters, 2017. **17**(12): p. 7897-7907.

24. S. Nakai, Y. Inoue, M. Hosomi, and A. Murakami, *Myriophyllum spicatum-released allelopathic polyphenols inhibiting growth of blue-green algae Microcystis aeruginosa.* Water Research, 2000. **34**(11): p. 3026-3032.

25. A. Crozier, I.B. Jaganath, and M.N. Clifford, *Phenols, Polyphenols and Tannins: An Overview*, in *Plant Secondary Metabolites*. 2006. p. 1-24.

26. G. Vázquez, E. Fontenla, J. Santos, M. Freire, J. González-Álvarez, and G. Antorrena, *Antioxidant activity and phenolic content of chestnut (Castanea sativa) shell and eucalyptus (Eucalyptus globulus) bark extracts.* Industrial crops and products, 2008. **28**(3): p. 279-285.

27. Y. Yilmaz and R.T. Toledo, *Major Flavonoids in Grape Seeds and Skins: Antioxidant Capacity of Catechin, Epicatechin, and Gallic Acid.* Journal of Agricultural and Food Chemistry, 2004. **52**(2): p. 255-260.

28. L.-L. Yang, C.-C. Wang, K.-Y. Yen, T. Yoshida, T. Hatano, and T. Okuda, *Antitumor activities of ellagitannins on tumor cell lines*, in *Plant Polyphenols 2*. 1999, Springer. p. 615-628.

29. S. Yoshizawa, T. Horiuchi, H. Fujiki, T. Yoshida, T. Okuda, and T. Sugimura, *Antitumor promoting activity of (−)-epigallocatechin gallate, the main constituent of "Tannin" in green tea.* Phytotherapy Research, 1987. **1**(1): p. 44-47.

30. H. Akiyama, K. Fujii, O. Yamasaki, T. Oono, and K. Iwatsuki, *Antibacterial action of several tannins against Staphylococcus aureus.* Journal of antimicrobial chemotherapy, 2001. **48**(4): p. 487-491.

31. T.-y. Wang, Q. Li, and K.-s. Bi, *Bioactive flavonoids in medicinal plants: Structure, activity and biological fate.* Asian Journal of Pharmaceutical Sciences, 2018. **13**(1): p. 12-23.

32. F. Melone, R. Saladino, H. Lange, and C. Crestini, *Tannin structural elucidation and quantitative 31P NMR analysis. 2. Hydrolyzable tannins and proanthocyanidins.* Journal of agricultural and food chemistry, 2013. **61**(39): p. 9316-9324.

33. P. Janeiro and A.M. Oliveira Brett, *Catechin electrochemical oxidation mechanisms.* Analytica Chimica Acta, 2004. **518**(1): p. 109-115.

34. D. Lin and B. Xing, *Tannic Acid Adsorption and Its Role for Stabilizing Carbon Nanotube Suspensions.* Environmental Science & Technology, 2008. **42**(16): p. 5917-5923.

35. M.L. Lehmann, R.M. Counce, R.W. Counce, J.S. Watson, N. Labbé, and J. Tao, *Recovery of Phenolic Compounds from Switchgrass Extract.* ACS Sustainable Chemistry & Engineering, 2018. **6**(1): p. 374-379.

36. F.E. Soetaredjo, S. Ismadji, S.P. Santoso, O.L. Ki, A. Kurniawan, and Y.-H. Ju, *Recovery of catechin and epicatechin from sago waste effluent: Study of kinetic and binary adsorption isotherm studies.* Chemical Engineering Journal, 2013. **231**: p. 406-413.

37. Y.A. Lee, J. Lee, D.W. Kim, C.-Y. Yoo, S.H. Park, J.J. Yoo, S. Kim, B. Kim, W.K. Cho, and H. Yoon, *Mussel-inspired surface functionalization of porous carbon nanosheets using polydopamine and Fe3+/tannic acid layers for high-performance electrochemical capacitors.* Journal of Materials Chemistry A, 2017. **5**(48): p. 25368-25377.

38. K.T. Sarang, X. Li, A. Miranda, T. Terlier, E.-S. Oh, R. Verduzco, and J.L. Lutkenhaus, *Tannic Acid as a Small-Molecule Binder for Silicon Anodes.* ACS Applied Energy Materials, 2020. **3**(7): p. 6985-6994.

39. J.Y. Oh, Y. Jung, Y.S. Cho, J. Choi, J.H. Youk, N. Fechler, S.J. Yang, and C.R. Park, *Metal–Phenolic Carbon Nanocomposites for Robust and Flexible Energy-Storage Devices.* ChemSusChem, 2017. **10**(8): p. 1675-1682.

40. P. Flouda, J. Yun, D. Loufakis, S.A. Shah, M.J. Green, D.C. Lagoudas, and J.L. Lutkenhaus, *Structural reduced graphene oxide supercapacitors mechanically enhanced with tannic acid.* Sustainable Energy & Fuels, 2020. **4**(5): p. 2301-2308.

41. M. Sevilla, N. Diez, G.A. Ferrero, and A.B. Fuertes, *Sustainable supercapacitor electrodes produced by the activation of biomass with sodium thiosulfate.* Energy Storage Materials, 2019. **18**: p. 356-365.

42. Y. Jia, L.-S. Xu, Y. Li, C.-L. Yao, and X.-J. Jin, *Synthesis and characterization of graphene/carbonized paper/tannic acid for flexible composite electrodes.* New Journal of Chemistry, 2018. **42**: p. 14576.

43. I.K. Ilic, A. Tsouka, M. Perovic, J. Hwang, T. Heil, F.F. Loeffler, M. Oschatz, M. Antonietti, and C. Liedel, *Sustainable Cathodes for Lithium-Ion Energy Storage Devices Based on Tannic Acid—Toward Ecofriendly Energy Storage.* Advanced Sustainable Systems. **n/a**(n/a): p. 2000206.

44. J. Lemieux, D. Bélanger, and C. Santato, *Toward Biosourced Materials for Electrochemical Energy Storage: The Case of Tannins.* ACS Sustainable Chemistry & Engineering, 2021.

45. S. Goriparti, M. Harish, and S. Sampath, *Ellagic acid–a novel organic electrode material for high capacity lithium ion batteries.* Chemical Communications, 2013. **49**(65): p. 7234-7236.

46. A.G. Pandolfo and A.F. Hollenkamp, *Carbon properties and their role in supercapacitors.* Journal of Power Sources, 2006. **157**(1): p. 11-27.

47. E. Fitzer, K.H. Köchling, H.P. Boehm, and H. Marsh, *Recommended terminology for the description of carbon as a solid.* Pure and Applied Chemistry, 1995. **67**(3): p. 473-506.

48. A. Hassani and A.R. Khataee, *Activated carbon fiber for environmental protection*. 2017: Elsevier Ltd. 245-280.

49. R.L. McCreery, *Advanced Carbon Electrode Materials for Molecular Electrochemistry.* Chemical Reviews, 2008. **108**(7): p. 2646-2687.

50. F. Béguin, V. Presser, A. Balducci, and E. Frackowiak, *Carbons and Electrolytes for Advanced Supercapacitors.* Advanced Materials, 2014. **26**(14): p. 2219-2251.

51. A. González, E. Goikolea, J.A. Barrena, and R. Mysyk, *Review on supercapacitors: Technologies and materials.* Renewable and Sustainable Energy Reviews, 2016. **58**: p. 1189-1206.

52. R.S. Kelly, D.J. Weiss, S.H. Chong, and T. Kuwana, *Charge-selective electrochemistry at high-surface-area carbon fibers.* Analytical Chemistry, 1999. **71**(2): p. 413-418.

53. A.L. Woodhead, M.L. de Souza, and J.S. Church, *An investigation into the surface heterogeneity of nitric acid oxidized carbon fiber.* Applied Surface Science, 2017. **401**: p. 79-88.

54. Q. Cheng, J. Tang, J. Ma, H. Zhang, N. Shinya, and L.-C. Qin, *Polyaniline-Coated Electro-Etched Carbon Fiber Cloth Electrodes for Supercapacitors.* The Journal of Physical Chemistry C, 2011. **115**(47): p. 23584-23590.

55. M. Li, H. Xiao, T. Zhang, Q. Li, and Y. Zhao, *Activated Carbon Fiber Derived from Sisal with Large Specific Surface Area for High-Performance Supercapacitors.* ACS Sustainable Chemistry & Engineering, 2019. **7**(5): p. 4716-4723.

56. L. Liu, Z. Niu, and J. Chen, *Flexible supercapacitors based on carbon nanotubes.* Chinese Chemical Letters, 2018. **29**(4): p. 571-581.

57. E. Frackowiak and F. Béguin, *Electrochemical storage of energy in carbon nanotubes and nanostructured carbons.* Carbon, 2002. **40**(10): p. 1775-1787.

58. D.N. Futaba, K. Hata, T. Yamada, T. Hiraoka, Y. Hayamizu, Y. Kakudate, O. Tanaike, H. Hatori, M. Yumura, and S. Iijima, *Shape-engineerable and highly densely packed single-walled carbon nanotubes and their application as super-capacitor electrodes.* Nature Materials, 2006. **5**(12): p. 987-994.

59. A. Peigney, C. Laurent, E. Flahaut, R.R. Bacsa, and A. Rousset, *Specific surface area of carbon nanotubes and bundles of carbon nanotubes.* Carbon, 2001. **39**(4): p. 507-514.

60. H. Yang, S. Kannappan, A.S. Pandian, J.H. Jang, Y.S. Lee, and W. Lu, *Graphene supercapacitor with both high power and energy density.* Nanotechnology, 2017. **28**(44).

61. Y. Wang, Z. Shi, Y. Huang, Y. Ma, C. Wang, M. Chen, and Y. Chen, *Supercapacitor Devices Based on Graphene Materials.* The Journal of Physical Chemistry C, 2009. **113**(30): p. 13103-13107.

62. M.D. Stoller, S. Park, Y. Zhu, J. An, and R.S. Ruoff, *Graphene-Based Ultracapacitors.* Nano Letters, 2008. **8**(10): p. 3498-3502.

63. M. Bacon, S.J. Bradley, and T. Nann, *Graphene Quantum Dots.* Particle & Particle Systems Characterization, 2014. **31**(4): p. 415-428.

64. Y.-J. Hsiao and L.-Y. Lin, *Enhanced Surface Area, Graphene Quantum Dots, and Functional Groups for the Simple Acid-Treated Carbon Fiber Electrode of Flexible Fiber-Type Solid-State Supercapacitors without Active Materials.* ACS Sustainable Chemistry & Engineering, 2020. **8**(6): p. 2453-2461.

65. J. Peng, W. Gao, B.K. Gupta, Z. Liu, R. Romero-Aburto, L. Ge, L. Song, L.B. Alemany, X. Zhan, G. Gao, S.A. Vithayathil, B.A. Kaipparettu, A.A. Marti, T. Hayashi, J.-J. Zhu, and P.M. Ajayan, *Graphene Quantum Dots Derived from Carbon Fibers.* Nano Letters, 2012. **12**(2): p. 844-849.

66. H.A.A. Bashid, H.N. Lim, S.M. Hafiz, Y. Andou, M. Altarawneh, Z.T. Jiang, and N.M. Huang, *Modification of carbon-based electroactive materials for supercapacitor applications*. 2018: Elsevier Inc. 393-413.

67. T. Tsubota, C. Wang, N. Murakami, and T. Ohno, *Effect of electrochemical treatment in H2SO4 aqueous solution on carbon material derived from cellulose with added guanidine phosphate.* Journal of Power Sources, 2013. **225**: p. 150–156.

68. R.L. McCreery and A.J. Bergren, *Surface Functionalization in the Nanoscale Domain*, in *Nanofabrication*. 2012. p. 163-190.

69. S.Y. Sayed, A. Bayat, M. Kondratenko, Y. Leroux, P. Hapiot, and R.L. McCreery, *Bilayer molecular electronics: all-carbon electronic junctions containing molecular bilayers made with "click" chemistry.* J Am Chem Soc, 2013. **135**(35): p. 12972-5.

70. M. Supur, S.R. Smith, and R.L. McCreery, *Characterization of Growth Patterns of Nanoscale Organic Films on Carbon Electrodes by Surface Enhanced Raman Spectroscopy.* Anal Chem, 2017. **89**(12): p. 6463-6471.

71. M. Supur, C. Van Dyck, A.J. Bergren, and R.L. McCreery, *Bottom-up, Robust Graphene Ribbon Electronics in All-Carbon Molecular Junctions.* ACS Appl Mater Interfaces, 2018. **10**(7): p. 6090-6095.

72. A.K. Farquhar, M. Supur, S.R. Smith, C. Dyck, and R.L. McCreery, *Hybrid Graphene Ribbon/Carbon Electrodes for High-Performance Energy Storage.* Advanced Energy Materials, 2018. **8**(35).

73. A.K. Farquhar, S.R. Smith, C.V. Dyck, and R.L. McCreery, *Large Capacity Enhancement of Carbon Electrodes by Solution Processing for High Density Energy Storage.* ACS Appl Mater Interfaces, 2020. **12**(9): p. 10211-10223.

74. R. Xu, A. Gouda, M.F. Caso, F. Soavi, and C. Santato, *Melanin: A Greener Route to Enhance Energy Storage under Solar Light.* ACS Omega, 2019. **4**(7): p. 12244-12251.

75. R.R. Mather, *Surface modification of textiles by plasma treatments*, in *Surface Modification of Textiles*, Q. Wei, Editor. 2009, Woodhead Publishing. p. 296-317.

76. M. Varga, T. Izak, V. Vretenar, H. Kozak, J. Holovsky, A. Artemenko, M. Hulman, V. Skakalova, D.S. Lee, and A. Kromka, *Diamond/carbon nanotube composites: Raman, FTIR and XPS spectroscopic studies.* Carbon, 2017. **111**: p. 54-61.

77. R. Al-Gaashani, A. Najjar, Y. Zakaria, S. Mansour, and M.A. Atieh, *XPS and structural studies of high quality graphene oxide and reduced graphene oxide prepared by different chemical oxidation methods.* Ceramics International, 2019. **45**(11): p. 14439-14448.

78. K.D. Vernon-Parry, *Scanning electron microscopy: an introduction.* III-Vs Review, 2000. **13**(4): p. 40-44.

79. D.G. Barrett, T.S. Sileika, and P.B. Messersmith, *Molecular diversity in phenolic and polyphenolic precursors of tannin-inspired nanocoatings.* Chemical Communications, 2014. **50**(55): p. 7265-7268.

80. P. van der Heide, *Introduction*, in *X-Ray Photoelectron Spectroscopy*. 2011. p. 1-12.

81. P. van der Heide, *XPS Instrumentation*, in *X-Ray Photoelectron Spectroscopy*. 2011. p. 27-60.

82. S. Brunauer, P.H. Emmett, and E. Teller, *Adsorption of Gases in Multimolecular Layers.* Journal of the American Chemical Society, 1938. **60**(2): p. 309-319.

83. K.S.W. Sing, *Adsorption methods for the characterization of porous materials.* Advances in Colloid and Interface Science, 1998. **76-77**: p. 3-11.

84. A. Galarneau, D. Mehlhorn, F. Guenneau, B. Coasne, F. Villemot, D. Minoux, C. Aquino, and J.-P. Dath, *Specific Surface Area Determination for Microporous/Mesoporous Materials: The Case of Mesoporous FAU-Y Zeolites.* Langmuir, 2018. **34**(47): p. 14134-14142.

85. N. Elgrishi, K.J. Rountree, B.D. McCarthy, E.S. Rountree, T.T. Eisenhart, and J.L. Dempsey, *A Practical Beginner's Guide to Cyclic Voltammetry.* Journal of Chemical Education, 2017. **95**(2): p. 197-206.

86. B.-A. Mei, O. Munteshari, J. Lau, B. Dunn, and L. Pilon, *Physical Interpretations of Nyquist Plots for EDLC Electrodes and Devices.* The Journal of Physical Chemistry C, 2018. **122**(1): p. 194-206.

87. S. Zhang and N. Pan, *Supercapacitors Performance Evaluation.* Advanced Energy Materials, 2015. **5**(6).

88. S. Song, F. Ma, G. Wu, D. Ma, W. Geng, and J. Wan, *Facile self-templating large scale preparation of biomass-derived 3D hierarchical porous carbon for advanced supercapacitors.* Journal of Materials Chemistry A, 2015. **3**(35): p. 18154-18162.

89. Y.S. Yun, M.H. Park, S.J. Hong, M.E. Lee, Y.W. Park, and H.-J. Jin, *Hierarchically Porous Carbon Nanosheets from Waste Coffee Grounds for Supercapacitors.* ACS Applied Materials & Interfaces, 2015. **7**(6): p. 3684-3690.

90. K. Fic, G. Lota, M. Meller, and E. Frackowiak, *Novel insight into neutral medium as electrolyte for high-voltage supercapacitors.* Energy & Environmental Science, 2012. **5**(2): p. 5842-5850.

91. S. Rahmanian, A.R. Suraya, R. Zahari, and E.S. Zainudin, *Synthesis of vertically aligned carbon nanotubes on carbon fiber.* Applied Surface Science, 2013. **271**: p. 424-428.

92. J. Peng, W. Gao, B.K. Gupta, Z. Liu, R. Romero-Aburto, L. Ge, L. Song, L.B. Alemany, X. Zhan, and G. Gao, *Graphene quantum dots derived from carbon fibers.* Nano letters, 2012. **12**(2): p. 844-849.

93. R. Gao, Z. Yuan, Z. Zhao, and X. Gao, *Mechanism of pyrogallol autoxidation and determination of superoxide dismutase enzyme activity.* Bioelectrochemistry and Bioenergetics, 1998. **45**(1): p. 41-45.

94. S.M. Siegel and B.Z. Siegel, *Autoxidation of Pyrogallol : General Characteristics and Inhibition by Catalase.* Nature, 1958. **181**(4616): p. 1153-1154.

95. T.S. Sileika, *Functional Biomaterials Inspired by Natural Polyphenols*, in *Biomedical Engineering*. 2014, Northwestern University: Evanston, Illinois.

96. T.S. Sileika, D.G. Barrett, R. Zhang, K.H.A. Lau, and P.B. Messersmith, *Colorless multifunctional coatings inspired by polyphenols found in tea, chocolate, and wine.* Angewandte Chemie - International Edition, 2013. **52**(41): p. 10766-10770.

97. Y. Xia, T.S. Mathis, M.Q. Zhao, B. Anasori, A. Dang, Z. Zhou, H. Cho, Y. Gogotsi, and S. Yang, *Thickness-independent capacitance of vertically aligned liquid-crystalline MXenes.* Nature, 2018. **557**(7705): p. 409-412.

98. V. Augustyn, J. Come, M.A. Lowe, J.W. Kim, P.L. Taberna, S.H. Tolbert, H.D. Abruña, P. Simon, and B. Dunn, *High-rate electrochemical energy storage through Li+ intercalation pseudocapacitance.* Nat Mater, 2013. **12**(6): p. 518-22.

99. Y. Wang, Y. Song, and Y. Xia, *Electrochemical capacitors: mechanism, materials, systems, characterization and applications.* Chemical Society Reviews, 2016. **45**(21): p. 5925-5950.

100. Z. Song, L. Miao, L. Li, D. Zhu, Y. Lv, W. Xiong, H. Duan, Z. Wang, L. Gan, and M. Liu, *A universal strategy to obtain highly redox-active porous carbons for efficient energy storage.* Journal of Materials Chemistry A, 2020. **8**(7): p. 3717-3725.

101. S. Jha, S. Mehta, Y. Chen, L. Ma, P. Renner, D.Y. Parkinson, and H. Liang, *Design and Synthesis of Lignin-Based Flexible Supercapacitors.* ACS Sustainable Chemistry & Engineering, 2020. **8**(1): p. 498-511.

102. X. Zhao, M. Gnanaseelan, D. Jehnichen, F. Simon, and J. Pionteck, *Green and facile synthesis of polyaniline/tannic acid/rGO composites for supercapacitor purpose.* Journal of Materials Science, 2019. **54**(15): p. 10809-10824.

103. K. Fic, A. Platek, J. Piwek, and E. Frackowiak, *Sustainable materials for electrochemical capacitors.* Materials Today, 2018. **21**(4): p. 437-454.